# Concatenated Entanglement Swapping Using Covariance Matrix Formalism


**Muhammad Asif**
**Regn. # 00000172991**

A thesis submitted in partial fulfilment of the requirements for the degree of
**Master of Science**
in
**Physics**

**Supervised by: Dr. Aeysha Khalique**

**Department of Physics**

School of Natural Sciences
National University of Sciences and Technology
H-12, Islamabad, Pakistan

2019

FORM TH-4

# National University of Sciences & Technology

## MS THESIS WORK

We hereby recommend that the dissertation prepared under our supervision by: Muhammad Asif, Regn No. 00000172991 Titled: Concatenated Entanglement Swapping Using Covariance Matrix Formalism be accepted in partial fulfillment of the requirements for the award of **MS** degree.

### Examination Committee Members

1. Name: DR. MUHAMMAD ALI PARACHA Signature: _____

2. Name: DR. RIZWAN KHALID Signature: _____

External Examiner: DR. RAMEEZ UL ISLAM Signature: _____

Supervisor's Name DR. AEYSHA KHALIQUE Signature: _____

_____ 27/9/2019
Head of Department Date

### COUNTERSINGED

Date: 27-9-19 _____
**Dean/Principal**

## THESIS ACCEPTANCE CERTIFICATE

Certified that final copy of MS thesis written by **Mr. Muhammad Asif**, Registration No. **00000172991**), of **School of Natural Sciences** has been vetted by undersigned, found complete in all respects as per NUST statutes/regulations, is free of plagiarism, errors, and mistakes and is accepted as partial fulfillment for award of MS/M.Phil degree. It is further certified that necessary amendments as pointed out by GEC members and external examiner of the scholar have also been incorporated in the said thesis.

Signature: Aysha Khalique

Name of Supervisor: Dr. Aeysha Khalique

Date: _____

Signature (HoD): _____

Date: 27/9/2019

Signature (Dean/Principal): _____

Date: 27-9-2019

*Dedicated*

*to*

*My Beloved Parents*

# Acknowledgements

All praise to Almighty Allah and His beloved Prophet Hazarat Muhammad (P.B.U.H.). I would like to express my sincere gratitude to my supervisor, Dr. Aeysha Khalique, whose guidance, and continuous encouragement and support right from the start to the end enabled me to successfully complete this work. I would like to express the deepest appreciation to my GEC member, Dr. Ali Paracha for helping me in understanding the problem and the relevant concepts. Also I would like to thank Dr. Naeem shahid, Dr. Shahid Iqbal and Mr. Ali for their valuable advices and suggestions. I take this opportunity to record my sincere thanks to all the faculty and staff members of SNS for providing valuable guidance always.

There is no words to thank my parents who supported me over the years and always inspired me. I offer gratitude to my brother Sohail Sarfaraz for being there always and for supporting me through out my life. I would like to recognize Adnan Khalique and Muhammad waqas for providing me help during my research work. These acknowledgments would not be complete without mentioning my friends: Basit Ali, Adnan Anjam, Muhammad Usman. I would like to thank them for their support and encouragement. I am pleased to have such jolly fellows who have always brought smile to my face.

# Abstract

In this dissertation, we use covariance matrix formalism to study three quantum information processes such as HOM interferometer, EPR interference and concatenated entanglement swapping. We studied Sagnac loop in detail as a source of entangled photons. We reviewed the Gaussian states i.e. vacuum state, coherent state and two mode sequeezed state. We discussed different important properties of Gaussian states and unitary operations that are very important in quantum information calculations. We started our study by developing covarience matrix from density matrix of any state. Covariance matrix reduces many complications in theoretical models. We also studied action af a Sagnac loop on a spontaneous parametric down conversion source state. In this dissertation we discussed dark counts, mode mismatch and channel losses. We calculated the visibilities for HOM interferometor, EPR Inerference. We focused on concatenated entanglement swapping, incorporating all kinds of channel losses and detector inefficiencies in our calculations for practical applications. We have developed a mathematica program for any general 'n' number of swapping. This program deals with beam spliter operation, Sagnac loop and other operations in generalized form.

# Contents

# List of Figures

# Chapter 1

# Introduction

Quantum information and computation involves the study of processes used for manipulating the information while making use of systems that obey laws of quantum physics. In physics, classical world provides an incomplete approximation to our underlying quantum facts. Facts like quantum interference and entanglement does not play any direct role in conventional information processing, they can provide basis, that helps to create unbreakable codes, and speed up intractable computations. Quantum Information Processing (QIP) deals with processing of information using quantum states of a system. From the last decade, quantum information has gain much attention of the scientific world in terms of improvement in data transfer security from one place to another. In some cases, it has been established that QIP can have more advantage to any known method of classical information processing. In contrast to classical methods a quantum computer can exponentially solve mathematical problems more accurately than any existing classical method. Quantum k Key Distribution (QKD) helps to share a random binary string which in principle unknown to any third member or Eve. Private communication through QKD is more secure under overhear including quantum computing. Information processing in classical system is carried out in the form of 0 or 1. Such processing is performed through classical bit that incorporates any physical quantity having two different values, e.g. the electrical potential (positive or negative voltages). While in QIP, quantum or classical information are carried out through quantum states. In addition, we apply quantum entangled states as a resource

to enhance the effective processing of quantum information. Therefore one can use single photon state as a quantum bit (qubit) while two photons entangled state, as a source for quamtum processing[4].

## 1.1 Qubit

In quantum information, data is represented in the form of qubit. A qubit plays a vital role in the development of quantum information theory, quantum computation, quantum games, quantum compelxity and quntum communication. A qubit may be considered as a supplement of a classical bit obtained from the appllication of the superposition principle. For a quantum mechanical system a qubit is defined as it is a superpostion state of $|0\rangle, |1\rangle$ which are mutually orthogonal and normalized. $|0\rangle, |1\rangle$ represent the state of a two level system. That is why by the supperposion of these two states one can easily describe a two level system. $|0\rangle$ will represent lower level and $|1\rangle$ will represnt upper level of a two level system. Two level system forms include up and down spins of an electron, an atom having excited or unexcited state and a photon with possible horizontal and vertical polarizations. So a theoratical qubit state can be defined as

$$|\Psi\rangle = c_0 |0\rangle + c_1 |1\rangle, \tag{1.1}$$

with $|c_0|^2 + |c_1|^2 = 1$. Now we write qubit state for photon, if a photon has horizontal $|H\rangle$ and vertical polariztion $|V\rangle$ then a photon qubit can be written as [4]

$$|\Psi\rangle = \alpha |H\rangle + \beta |V\rangle, \tag{1.2}$$

again with $|\alpha|^2 + |\beta|^2 = 1$. When a measurement is done on a supperposion state the atom found in its specific stae but before measurement no one can tell us that in which state electron , atom or a polarization photon is in space. It is all about measurements that play a vital role in Information process. It means that state vector will correspond to some specific state, but no more remain in supperposion state. So after measurement by applying again measurement we cannot get information about state.

## 1.2 Entanglement

Scientists put a great attention on quantum entanglement as it is considered a vital source for quantum communication and information processing. In 1935 Einstein, Podolsky and Rosen supposed an experiment that described the incompletness of quantum mechanics theory. This experiment is called as EPR paradox. According to EPR paradox their is a hidden variable within a particle that reveals its properties during a measurement. But after many experiment it was understood that two particles can interact with each other and they cannot behave independently. Such interacting particles are called as entangled particles and this phenomenon of long distance interaction is called entanglement. Entanglement is the basic property of quantum systems that can be occur between different particles or withintwo or more degree of freedom of a single particle. In classical world there is no concept of entanglement between different particles that are distance part, but is quantum mechance particles are entangled even if they are distance apart [5].

An etangled state is described a state which cannot be written as a tensor product state. It can not separated into state of system A and B. Consider Alice with states $|0\rangle_A, |1\rangle_A$ and Bob with state $|0\rangle_B, |1\rangle_B$ then entangled state of Alice and Bob can be defined as

$$|\Psi\rangle = \frac{|1\rangle_A |0\rangle_B + |0\rangle_A |1\rangle_B}{\sqrt{2}}, \tag{1.3}$$

if $|H\rangle$ is a horizontal polarization and $|V\rangle$ is a vertical polarization of a photon then entangle state in terms of polarization of photons can be written as

$$|\Psi\rangle_{1,2} = \frac{|H_1\rangle |V_2\rangle + |V_1\rangle |H_2\rangle}{\sqrt{2}}, \tag{1.4}$$

When we perform a measurement on photon 1 and find photon to be localized in horizontal polariztion state, as a result we can immedietly guess the photon 2 will be in vertical polarization and vice versa. This is due to the superposition of quantum states which makes the outcome of measurement completely random. This means that before a measurement we cannot know about the outcome of the event. This means that if a photon 1 is collapsed in state $|V\rangle_1$ or $|H\rangle_1$ then photon 2 will automatically

will collapes in $|V\rangle_2$ or $|H\rangle_2$ [6].
Dense coding, quantum key distribution and teleportation become possible due to realem of quantum entanglement. We will discuss entangalement swapping in detail in chapter 3.

## 1.3 Spontanous Parametric Down Conversion Souces

The first experiment for polarization-entangled photon pair source was conducted with atomic-cascade decays to violate remote Bell inequality. In the beginning of 1987 entangled photons were observed from a nonlinear crystal that is pumped with a intense coherent source. So it is clear that nonlinear crystal have noval importance in most engtnaled sources [7].
Spontaneous Parametric Down Conversion (SPDC) is a strongest method leading to the emission of photon pair from nonlinear crystal. It is a process in with three waves mix togather with the help of nonlinear crystal of susceptibility $\chi^{(2)}$. The phenomenon of SPDC first intoduced in 1961 by Louisell and his co-worker [8]. In general SPDC is a process in which a single photon decays into two lower energy daughter photons. The theory of SPDC was developed by Kleiman and modern mechanical clculations was developed by by Hong and Mandel in 1985 [9].

### 1.3.1 Basic principle of SPDC source

Spontaneous parametric downconversion source is based on three waves in which photon from source is passed through a nonlinear optical crystal that has a equal probabaility to be converted into daughter photons. We assumed that it is a three plane wave mixing. It has two types that are called type I and type II downconversion. In SPDC process daughter photons are characterised by their polarization from crystal axis and are called ordinary and extraordinary. In nonlinear optics the downconverted photons are called signal photons (index s) and idler photon (index i).
Polarization direction of signal and idler modes for type I downconverion is identical. It means that if the pump have a extraordinary polarization then signal and idler will be

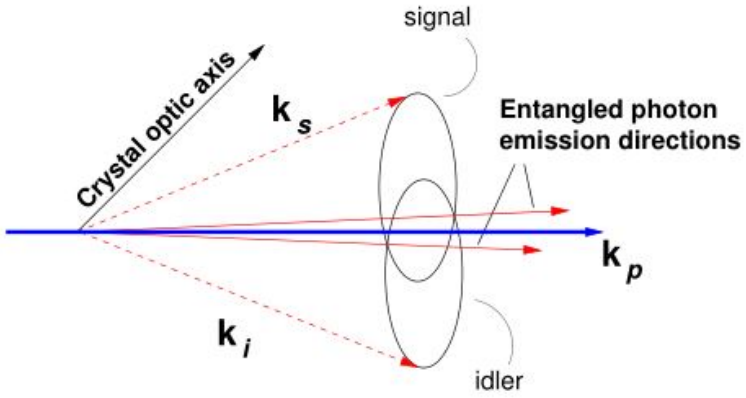


Figure 1.1: Signal and idler mode for spontaneous parametric down convervion source [1].

in ordinary polarization. The outcome of type-I down-conversion is squeezed vaccum that contains even number photon. The degenerate twin photons are emitted as cones in type II down-conversion. In laborartoray frame we refer exteraordinary photon with vertical polarization $|V\rangle$.

The frequencies of three field are expressed as $\omega_{p,s,i}$ and vectors of their fields are written as $k_{p,s,i}$. The energy and momentum conversion can be written as

$$\omega_p = \omega_s + \omega_i, \tag{1.5}$$

$$k_p = k_s + k_i, \tag{1.6}$$

One cone contains ordinary polarized photons and other contains extra ordinary polarized photons. The opening angle of photon relies on the angle of optical axis with pump field and written as $\theta_p$. At some value of of $\theta_p$, we get degenerate emission of photons . This will happen when two cones exactly overlap at one point. The emission of photons is in the direction of original photon. When $\theta_p$ is increased, two cones come close and interact at two points having pump beam in center. Photons coming through these points are completly indistingishable excluding polarization states. So

two possible indistinguisable decay path available at these interaction and causes the emission of polarized entangled state. The emitted state can be written as

$$|\psi\rangle = \frac{(|H_1, V_2\rangle + e^{i\phi}\,|H_2 V_1\rangle)}{\sqrt{2}}, \tag{1.7}$$

$\phi$ is a phase angle between ordinary and extraordinary polarized light introduced by the crystal birefringence. Global phase may be ignored. In addition to realtive phase, the crystal also introduce longitudinal and transvers walk-off. In longitudinal walk-off ordinary and extraordinary have different speeds throughout and easily distingishable from each other. For transver walk-off ordinary and extraordinary waves propagate in different directions and are separeted after passing through the down conversion crystal. After the walk-offs are corrected, one of the four maximally entangled Bells states can be obtained by using half wave plate and quarter wave in the source route [10].

$$\left|\psi^{\pm}\right\rangle = \frac{(|H_1, V_2\rangle \pm |H_2, V_1\rangle)}{\sqrt{2}}, \tag{1.8}$$

$$\left|\phi^{\pm}\right\rangle = \frac{(|H_1, H_2\rangle \pm |V_1, V_2\rangle)}{\sqrt{2}}, \tag{1.9}$$

above four state have noval importance and have been used in many quantum information theoretical models such as quantum teleportation.

## 1.4 Bell States and Bell Measurment

### 1.4.1 Bell States

First time the concept of Bell sates was given by John, S Bell'. These states are called maximally entangled states. If we have two entangled photons in horizontal and vertical polarization, it means that by knowing polarization state of one photon then we can guess the polarization state of the second photon. For two qubit system the maximally entangled Bell states can be written as

$$\left|\psi^{+}_{1,2}\right\rangle = \frac{(|H_1, V_2\rangle + |V_1, H_2\rangle)}{\sqrt{2}}, \tag{1.10}$$

$$\left|\psi^{-}_{1,2}\right\rangle = \frac{(|H_1, V_2\rangle - |V_1, H_2\rangle)}{\sqrt{2}}, \tag{1.11}$$

$$\left|\phi^{+}_{1,2}\right\rangle = \frac{(|H_1, H_2\rangle + |V_1, V_2\rangle)}{\sqrt{2}}, \tag{1.12}$$

$$\left|\phi^{-}_{1,2}\right\rangle = \frac{(|H_1, H_2\rangle - |V_1, V_2\rangle)}{\sqrt{2}}. \tag{1.13}$$

A above Bell states have a marvalous properties. Some of them are given blew →.
Bell states form a orthogonal basis in two qubit Hilbert Space and any pure state is described by supperposition of Bell states.
→ The Bell states are only symmtrics and antisysmmtric with respect two permutations of subsystem.
→ The antisysmmetric state s$\left|\phi^{-}_{1,2}\right\rangle$ dilivers perfect rationally invariant exclusive [11].

### 1.4.2 Bell Measurement

Bell-state measurement can be described as a two-qubit projection on Bell states that are maximally entangled. By using Bell measurement we can ditinguished between some Bell states. For example we can distinguished between $|\psi^{-}\rangle$ and $|\psi^{+}\rangle$ but we cannot differentiate between $|\phi^{-}\rangle$ and $|\phi^{+}\rangle$. It is a main process in many quantum phenomenon such as teleportation and entanglement swapping. There are many types of Bell-state measurement. Here we will discuss linear optical method of Bell-state measurement.

If r is the reflectance and t is transmittance of a beam splitter, then for $50:50$ beam splitter $\mid r \mid$ and $\mid t \mid$ are $\frac{1}{\sqrt{2}}$. Let I, R and T be the amplitude of incident, reflected and transmitted beams respectively then from classical mechanics.

$$R = rI, \tag{1.14}$$

$$T = tI, \tag{1.15}$$

If we assume that beam splitter is lossless then we have a relation

$$\mid I \mid^2 = \mid R \mid^2 + \mid T \mid^2, \tag{1.16}$$

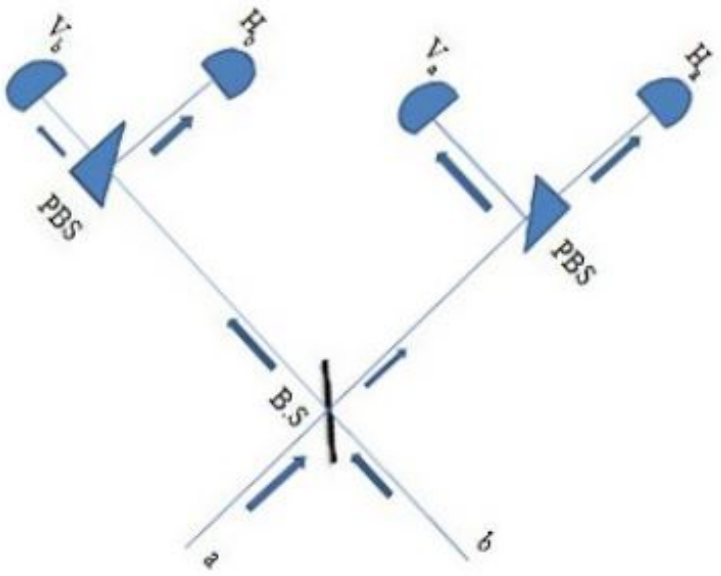


Figure 1.2: Bell-state analyzer. This Shows that one photon is on path a and other on path b incident on 50 : 50 beam splitter where thy interact with each other and are reflected or transmitted from the beam splitter. Finally they reached upon polarization beam splitter which transmits or reflects photon depending upon polarization.

which is possible if

$$| r |^2 + | t |^2 = 1, \tag{1.17}$$

Working in quantum mechanics we replace complex amplitudes of beams by their respective annhilation operators $\hat{a}_k$ where (k = i, r, t). In quantum mechanics we have relations just like classical mechanics that are

$$\hat{a}_r = r\hat{a}, \tag{1.18}$$

$$\hat{a}_t = t\hat{a}, \tag{1.19}$$

These operators should obey the following commutation relation

$$\left[\hat{a}_k, \hat{a}_l^\dagger\right] = \delta_{k,l}, \tag{1.20}$$

$$[\hat{a}_k, \hat{a}_l] = 0, \tag{1.21}$$

$$\left[\hat{a}_k^\dagger, \hat{a}_l^\dagger\right] = 0, \tag{1.22}$$

As above operators do not follow the commutation relations, so they cannot give complete describtion of quantum mechanics of beam splitter. In quantum mechanics we cannot leave any port empty. If there is no photon on any port then we consider vacuum on that port in quantum mechanics. So beam splitter action on operators can be written as

$$\begin{aligned} \hat{a}_r &\xrightarrow{\hat{U}_B} \frac{\hat{a}_i + i\hat{a}_o}{\sqrt{2}}, \\ \hat{a}_t &\xrightarrow{\hat{U}_B} \frac{i\hat{a}_i + \hat{a}_o}{\sqrt{2}}, \end{aligned} \tag{1.23}$$

Where $\hat{a}_o$ is a operetor for vacuum [2].

Here for 50 : 50 beam splitter is used for measurement. Two entangled photons in spatial modes enter in beam splitter through port a and b and leave the 50 : 50 beam splitter, as illustrated in Fig. 1.2 above. By using this scheme one can separate and identify each Bell state as mentioned in [ref]. The antisymmetric $|\psi^-\rangle$ state is completly distiguished and identified when output of photons appear on the different beam splitter ports. In case of $|\psi^+\rangle$ state, photons appear on the same port of the detector and these emerging photons still have horizontal and vertical polrization components. To identified $|\psi^+\rangle$ completly a polarization beam spliiter (PBS) is added after beam spliter , so emerging photons will appear on different ports of the polarizer. when the photon appears on either beam splitter output ports and photon emerge on different ports of the polarization beam splitter then $|\psi^-\rangle$ is observed i.e. either the detectors $c_h$ and $d_v$ click, or $c_v$ and $d_h$ . On the other hand, if two photons come out from same beam splitter port and emerge on different polarization beam splitter ports then $|\psi^+\rangle$ will be observed i.e either $c_h$ and $c_v$ click, or $d_h$ and $d_v$ . Here we follow the HVVH sequence of the detector for modes a and b then state $|\psi^-\rangle$ is written as

$$\left|\psi^-\right\rangle = \frac{1}{2}[|0101\rangle - |1010\rangle], \tag{1.24}$$

$$\left|\psi^-\right\rangle = \frac{1}{2}[\hat{a}_v^\dagger \hat{b}_h^\dagger |0000\rangle - \hat{a}_h^\dagger \hat{b}_v^\dagger |0000\rangle]. \tag{1.25}$$

Now applying beam splitter transformations, above equation will become

$$\left|\psi^-\right\rangle = \frac{1}{2}\left[\frac{(\hat{a}_v^\dagger + \iota\hat{b}_v^\dagger)(\iota\hat{a}_h^\dagger + \hat{b}_h^\dagger)}{2}|0000\rangle - \frac{(\hat{a}_h^\dagger + \iota\hat{b}_h^\dagger)(\iota\hat{a}_v^\dagger + \hat{b}_v^\dagger)}{2}|0000\rangle\right], \tag{1.26}$$

$$= \frac{1}{2\sqrt{2}}\Big[(\iota\hat{a}_v^\dagger\hat{a}_h^\dagger+\hat{a}_v^\dagger\hat{b}_h^\dagger-\hat{b}_v^\dagger\hat{a}_h^\dagger+\iota\hat{b}_v^\dagger\hat{b}_h^\dagger)\,|0000\rangle-(\iota\hat{a}_h^\dagger\hat{a}_v^\dagger+\hat{a}_h^\dagger\hat{b}_v^\dagger-\hat{b}_h^\dagger\hat{a}_v^\dagger+\iota\hat{b}_h^\dagger\hat{b}_v^\dagger)\,|0000\rangle\Big], \quad (1.27)$$

$$\big|\psi^-\big\rangle = \frac{1}{2\sqrt{2}}\Big[\iota\,|1100\rangle+|0101\rangle-|1010\rangle+\iota\,|0011\rangle-\iota\,|1100\rangle-|1010\rangle+|0101\rangle-\iota\,|0011\rangle\Big], \quad (1.28)$$

$$\big|\psi^-\big\rangle = \frac{1}{\sqrt{2}}\Big[\,|0101\rangle-|1010\rangle\,\Big]. \quad (1.29)$$

Here above equation shows that photons appeared on different output ports of the beam splitter.

Now for $|\psi^+\rangle$

$$\big|\psi^+\big\rangle = \frac{1}{2}[|0101\rangle+|1010\rangle], \quad (1.30)$$

$$\big|\psi^+\big\rangle = \frac{1}{2}[\hat{a}_v^\dagger\hat{b}_h^\dagger\,|0000\rangle+\hat{a}_h^\dagger\hat{b}_v^\dagger\,|0000\rangle]. \quad (1.31)$$

Now applying beam splitter transformations, above equation will become

$$\big|\psi^+\big\rangle = \frac{1}{2}\Big[\frac{(\hat{a}_v^\dagger+\iota\hat{b}_v^\dagger)(\iota\hat{a}_h^\dagger+\hat{b}_h^\dagger)}{2}\,|0000\rangle+\frac{(\hat{a}_h^\dagger+\iota\hat{b}_h^\dagger)(\iota\hat{a}_v^\dagger+\hat{b}_v^\dagger)}{2}\,|0000\rangle\Big], \quad (1.32)$$

$$= \frac{1}{2\sqrt{2}}\Big[(\iota\hat{a}_v^\dagger\hat{a}_h^\dagger+\hat{a}_v^\dagger\hat{b}_h^\dagger-\hat{b}_v^\dagger\hat{a}_h^\dagger+\iota\hat{b}_v^\dagger\hat{b}_h^\dagger)\,|0000\rangle+(\iota\hat{a}_h^\dagger\hat{a}_v^\dagger+\hat{a}_h^\dagger\hat{b}_v^\dagger-\hat{b}_h^\dagger\hat{a}_v^\dagger+\iota\hat{b}_h^\dagger\hat{b}_v^\dagger)\,|0000\rangle\Big], \quad (1.33)$$

$$\big|\psi^+\big\rangle = \frac{1}{2\sqrt{2}}\Big[\iota\,|1100\rangle+|0101\rangle-|1010\rangle+\iota\,|0011\rangle+\iota\,|1100\rangle+|1010\rangle-|0101\rangle+\iota\,|0011\rangle\Big], \quad (1.34)$$

$$\big|\psi^+\big\rangle = \frac{\iota}{\sqrt{2}}\Big[\,|1100\rangle+|0011\rangle\,\Big]. \quad (1.35)$$

From above it is clear that emerging photons will appear at different ports of beam splitter. Now consider $|\phi^\pm\rangle$ states

$$\big|\phi^\pm\big\rangle = \frac{1}{\sqrt{2}}\Big[\,|1001\rangle\pm|0110\rangle\,\Big], \quad (1.36)$$

$$\big|\phi^\pm\big\rangle = \frac{1}{\sqrt{2}}\Big[\hat{a}_h^\dagger\hat{b}_h^\dagger\,|0000\rangle\pm\hat{a}_v^\dagger\hat{b}_v^\dagger\,|0000\rangle\,\Big], \quad (1.37)$$

$$\big|\phi^\pm\big\rangle = \frac{1}{2}\Big[\frac{(\hat{a}_h^\dagger+\iota\hat{b}_h^\dagger)(\iota\hat{a}_h^\dagger+\hat{b}_h^\dagger)}{2}\,|0000\rangle\pm\frac{(\hat{a}_v^\dagger+\iota\hat{b}_v^\dagger)(\iota\hat{a}_v^\dagger+\hat{b}_v^\dagger)}{2}\,|0000\rangle\Big], \quad (1.38)$$

for $|\phi^+\rangle$ state

$$\left|\phi^+\right\rangle = \frac{1}{2\sqrt{2}}\Big[(\iota\hat{a}_h^\dagger\hat{a}_h^\dagger + \hat{a}_h^\dagger\hat{b}_h^\dagger - \hat{b}_h^\dagger\hat{a}_h^\dagger + \iota\hat{b}_h^\dagger\hat{b}_h^\dagger)\,|0000\rangle + (\iota\hat{a}_v^\dagger\hat{a}_v^\dagger + \hat{a}_v^\dagger\hat{b}_v^\dagger - \hat{b}_v^\dagger\hat{a}_v^\dagger + \iota\hat{b}_v^\dagger\hat{b}_v^\dagger)\,|0000\rangle\Big], \tag{1.39}$$

$$\left|\phi^+\right\rangle = \frac{1}{2\sqrt{2}}\Big[(\iota\sqrt{2}\,|2000\rangle + |1001\rangle - |1001\rangle + \iota\sqrt{2}\,|0002\rangle + \iota\sqrt{2}\,|0200\rangle + |0110\rangle - |0110\rangle + \iota\sqrt{2}\,|0020\rangle\Big], \tag{1.40}$$

$$\left|\phi^+\right\rangle = \frac{\iota}{2}\Big[(|2000\rangle + |0002\rangle + |0200\rangle + |0020\rangle\Big]. \tag{1.41}$$

Now for for $|\phi^-\rangle$ state

$$\left|\phi^-\right\rangle = \frac{1}{2\sqrt{2}}\Big[(\iota\sqrt{2}\,|2000\rangle + |1001\rangle - |1001\rangle + \iota\sqrt{2}\,|0002\rangle - \iota\sqrt{2}\,|0200\rangle - |0110\rangle + |0110\rangle - \iota\sqrt{2}\,|0020\rangle\Big], \tag{1.42}$$

$$\left|\phi^-\right\rangle = \frac{\iota}{2}\Big[(|2000\rangle + |0002\rangle - |0200\rangle - |0020\rangle\Big]. \tag{1.43}$$

We see that for both $|\phi^+\rangle$ and $|\phi^-\rangle$ both photons end up on same direction. So these states can not be distinguished. Thus this optical Bell measurement can distinguished between only $|\psi^+\rangle$ and $|\psi^-\rangle$ state.

## 1.5 Sagnac loop

Using Type-I and Type-II matching as mentioned above, SPDC source can be used to generate entangled photon states. Due to the random occurrence of entangled photons in coherence length, continuous wave (cw) based pumped SPDC sources are not helpful in the quantum computing. Using femetosecond laser as a source can resolve this problem. When we use ultrashot pulse laser with type-II SPDC, it gives very poor correlation than cw-laser.

One of the most latest technique based on interferometer used to produce entangled photon pairs is called Sagnac loop. This is independent from the thickness of crystal and insensititve of bandwith of filter. Sagnac loop shows great stability in quantum information experiments.

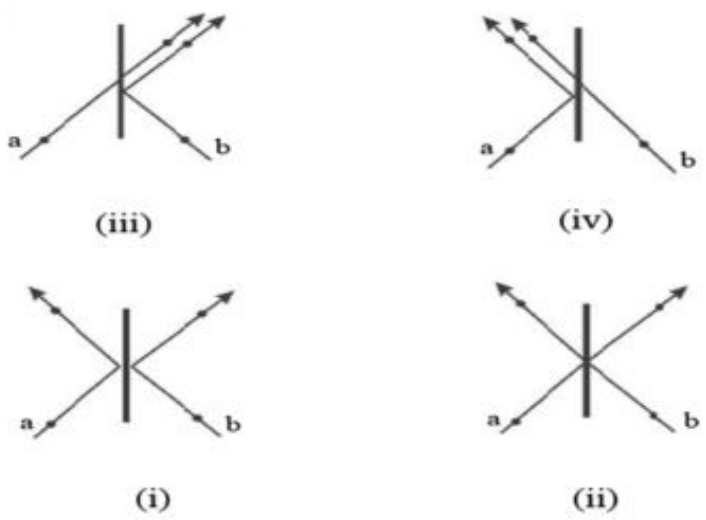


Figure 1.3: Shows possible outcome of a 50 : 50 beam splitter. In case (i) both photons are reflected from beam splitter. In case (ii) both coming photons are transmitted through beam splitter.In case (iii) photon in path a is transmitted while a photon in path b is reflected.In casse (iv) photon in path b is transmitted while a photon in path a is reflected

### 1.5.1 Scheme Of Sagnac Loop

A simplified Sagnac loop consist of a round trip and a 50 : 50 beam splitter as shown in figere 1.4. When a light comes at beamsplitter, it divides the light into equal halves. First half starts travelling clockwise while second half travels counter clockwise in the loop. After travelling some distance in loop these waves arrive on beam splitter again. For moderate range Sagnac loop, time based interaction with environment are very limited and environment equally affects both halves of loop. This means that clockwise and counter clockwise ars compensated that they have equal lengths. Phase difference between clockwise and anticlockwise loop is maintained that causes a stable interference.

When a nonlinear crystal with half wave plate (HWP) $\lambda/2$ at $45^\circ$ is introduced in path of Sagnac loop then entangled photons are produced. The HWP $\lambda/2$ corresponds to light frequency $\omega$ and wave plate $\lambda$ corresponds to light frquency $2\omega$. When light

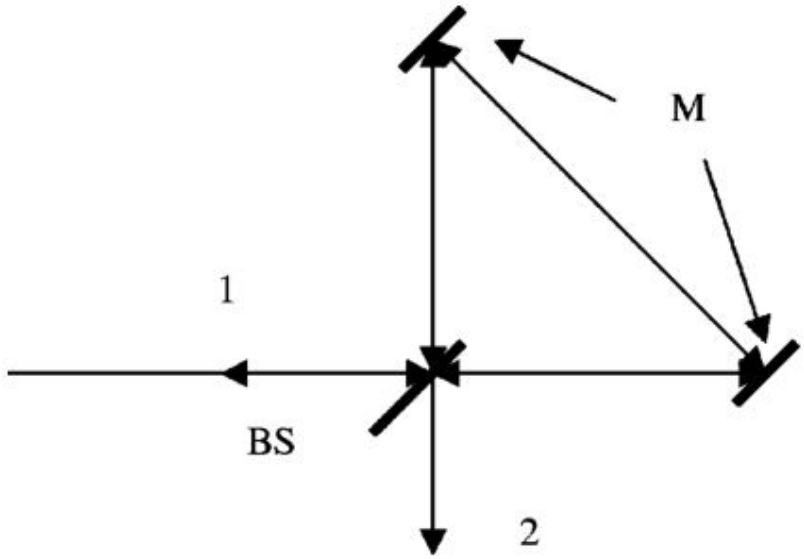


loop.jpg

Figure 1.4: Scheme for sagnac loop consisting on beam splitter and mirrors

from a pump of frequency $2\omega$ reaches at beam splitter then half light is transmitted through the beam splitter and moves towords the nonlinear crystal and have a horizontal polarization $|2H\rangle$. Polarization pair after passing through the nonlinear crystal, is tiwisted vertically that is $|2V\rangle$. The reflected portion of beam produces horizontal polarization pair of photon which is mixed at beam splitter with $|2V\rangle$. If we study one photon in each port of beam spliter then we get a polarized entangled photon pair $|HH\rangle_{1,2} + |VV\rangle_{1,2}$, where indices 1,2 stand for output of beam splitter [12].

## 1.6 Entanglement Swapping

Entanglement is produced either by two entangled photons through single source or by two particles interacting with each other. In addition, Entanglements is also achieved by using the projection of two particles on the entangled state. It implies that entanglement swapping is produced from the measurement of the projection and it does not involve two particles to interact directly. When one of two particles are entangled with another partner particle, a suitable measurement i.e. Bell measurement, of the partner

particle will cause entanglement between rest of the particles. This phenomenon is called entanglement swapping. In quantum key distribution entanglement swapping between photon pairs is basically used for long distance communication.

### 1.6.1 Scheme For Entanglement Swapping

The basic setup for entanglement swappimg consists of two parametric down conversion sources, a Bell measurment equipments with four dectectors. The two PDC sources emit four photons in the form of pairs, each photon correspond to a spatial mode. The photons a and b spatial mode corresponds to first PDC source whereas photon in spatial mode c and d correspond to second PDC mode as shown in fig 1.5. As photon in mode a and b are entangled with each other and similarly photons in spatial mode c and d are entangled with each other. Here is our task to shift entanglement between a and d spatial mode. For entanglement swapping, joint Bell measurement is applied on b and c mode that shifts entanglement between a and d that are not in direct connection. Thus, the previous entanglement between a and b and the photon pairs c and d is switched to the photon pair a and d.
Now if we have a polarized qubits and a Bell state calculations is applied on b and c mode of the PDC sources and output of beam splitter $b^{'}$ and $c^{'}$ are move towards the polarizing beam splitter and finally collected four states $c^{'}_{H}$, $c^{'}_{V}$, $b^{'}_{H}$, $b^{'}_{V}$ at four detectors. The counts of detectors are labled as (qrst). As polarizing beamsplitter allows horizontal component of polarization to pass through and blocks vertical component of the polarization. The output signal q attribute to $c^{'}_{H}$, out r belongs to $c^{'}_{V}$ mode, s shows $b^{'}_{V}$ mode and t refers to $b^{'}_{H}$ mode [13].

The concept of entanglement swapping is extended in the form of cancatenated entanglement swapping. Concatenated entanglement swapping is a chain of Bell measurements on photon sources to swapping entanglemnt between different modes. Concatenated entanglement swapping is useful in long distance quantum key distribution and used to overcome environment effects and improve stability.

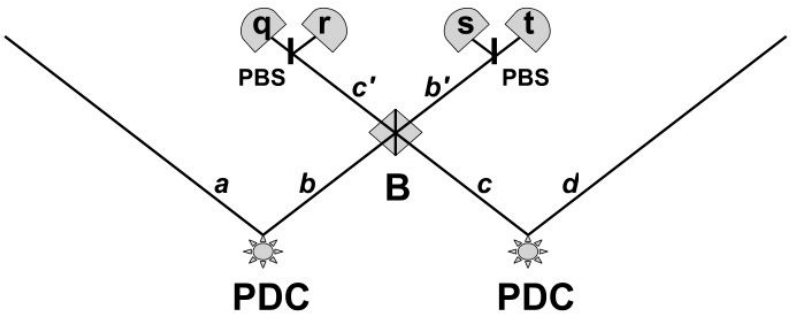


Figure 1.5: Photon-polarization qubit swapping setup comprises of two parametric down conversion sources (PDC) and a Bell measurement with four detectors

## 1.7 Thesis Outline

In this thesis, we review the multiphton pair effects in spontaneous parametric down conversion based photonic quantum information processing [3] and how it can become useful to increase range of communication in concatenated entanglement swapping.
In chapter 2, we discuss Gaussian states as a lasser source. We discuss and review different types of Gaussian states such as vacuum state, coherent states,one mode sequeezed state and two mode sequeezed vacuum state. We discussed mathematical description of coherent stete and expressed it in form of number states. We also developed state representation for two mode sequeezed state. We discussed how we can developed covariance matrix from given state and also we discussed characteristics function approach. We discussed some novel charactristices of Gaussion states. At the end of second chapter we give a look on the different unitary operation for Gaussion states. We develop matrix form of the beam splitter operation and for polarizers.
In chapter 3, we apply our covariance matrix approach on Hong O Mandle interferometer and calculate its visibility that completly agrees with previous results. We explain EPR interferometor using covariance matix of two mode sequeezed state. We apply Sagnac loop and calculate all mathematical steps in detail. Finally we apply covariance matrix approach with sagnac loop source on concatenated entanglement swapping. We calculate visibility by incorporating all channel losse and detector inefficiences and plot

graphs between visibility and avarege no of photons with general program.
In chapter 4, we conclude our thesis.
In appendix we put our general program.

# Chapter 2

# Gaussian States

In this chapter we will discuss about Gaussian states, types of Gaussion state mathematical description of Gaussion states, characteristic function approach, establish a covariance matrix from state and Gaussioan operations. In Sec. 2.1, we briefly discuss intoduction of Gaussian in quantum information. In Sec. 2.2, we discuss vacuum state and develop its characteristic function. In Sec. 2.3, we discuss coherent states and expressed it in fock basis. In Sec. 2.4, we mathematically described one mode sequeezed vacuum state and also represent its final stae in form of number states. In Sec. 2.5, we review two mode sequeezed vacuum state. In Sec. 2.6, we give detail on covariance matrix, we give its general formula and its general form. We calculate covariance matrix for various states such as vacuum state and coherent state. In Sec. 2.7, we discuss some important unitary opreation for Guassion states.

## 2.1 Introduction

It is important question how one can fetch quantum states for practicle communication system. In practice, it is a very difficult task to produce the single photon states or two-photon entangled states. The state of the light coming from a lasser light is called Gaussian coherent state. Vacuum state and sequeezed vacuum states are also charactrized as Gaussian states. A state is Gaussian mathematically if its phase space distribution function or its Fock space density operator is in Gaussian form. Gaussian

states are of supreme important in number of quantum information expriment. All important experiments of quantum information are performed with Gaussian light [4].

## 2.2 Vacuum State

One important example of Gaussian state is a vacuum state. The vacuum state is defined as $|0\rangle$. The density operator is $|0\rangle\langle 0|$. The vacuum state's characteristic function is calculated as

$$\chi(\zeta_1,\zeta_2) = Tr\{e^{\zeta_1\hat{x}+\zeta_2\hat{p}}\,|0\rangle\langle 0|\} = \sum_{0}^{\infty}\langle n|\, e^{\zeta_1\hat{x}+\zeta_2\hat{p}}\,|0\rangle\langle 0|n\rangle = \langle 0|\, e^{\zeta_1\hat{x}+\zeta_2\hat{p}}\,|0\rangle \tag{2.1}$$

with $\hat{x} = (\hat{a}^\dagger + \hat{a})/\sqrt{2}$ and $\hat{p} = i(\hat{a}^\dagger - \hat{a})/\sqrt{2}$

$$e^{\zeta_1\hat{x}+\zeta_2\hat{p}} = e^{(i\zeta_1-\zeta_2)\hat{a}^\dagger/\sqrt{2}+(i\zeta_1+\zeta_2)\hat{a}/\sqrt{2}} = e^{-(\zeta_1^2+\zeta_2^2)/4}e^{(i\zeta_1-\zeta_2)\hat{a}^\dagger/\sqrt{2}}e^{(i\zeta_1+\zeta_2)\hat{a}/\sqrt{2}} \tag{2.2}$$

by further simplification we get

$$\chi(\zeta_1,\zeta_2) = e^{-(\zeta_1^2+\zeta_2^2)/4} = exp^{-1/4(\zeta_1,\zeta_2)\gamma_o\begin{bmatrix}\zeta_1\\ \zeta_2\end{bmatrix}}. \tag{2.3}$$

Eq. 2.3 shows that vacuum state has a Gaussian characteristic funtion, $\gamma_o$ is $2\times 2$ covariance matrix.

## 2.3 Coherent State

Coherent states give the accurate value of the electric field expectation with vacuum fluctuations so these states are classical like states. We can get non-zero expectation value of the $\hat{a}$ and $\hat{a}^\dagger$ operators by using superposition of number states differed only by $\pm$ 1. Superposion of the number states will help to get non zero ecpectation value of $\hat{a}$ operator. If these states are the eigenstates of the $\hat{a}$ operator then [2].

$$\hat{a}\,|\alpha\rangle = \alpha\,|\alpha\rangle\,, \tag{2.4}$$

where $\alpha$ is a complex number, it is a eigenvalue of $\hat{a}$ opreator. The state $|\alpha\rangle$ is right eigenstate of $\hat{a}$ and state $\langle\alpha|$ is left eigenstate of $\hat{a}^\dagger$ with eigenvalue $\alpha^*$.

$$\langle\alpha|\,\hat{a}^\dagger = \langle\alpha|\,\alpha^*, \tag{2.5}$$

So we can expand $|\alpha\rangle$ in terms of number state $|n\rangle$ as

$$|\alpha\rangle = \sum_{n=0}^{\infty} C_n\,|n\rangle \tag{2.6}$$

The action of $\hat{a}$ on $|\alpha\rangle$ can be written as

$$\hat{a}\,|\alpha\rangle = \sum_{n=1}^{\infty} C_n\sqrt{n}\,|n-1\rangle = \alpha\sum_{n=0}^{\infty} C_n\,|n\rangle\,. \tag{2.7}$$

By comparing coefficient of $|n\rangle$ on both sides we have

$$C_n\sqrt{n} = \alpha C_{n-1} \tag{2.8}$$

$$C_n = \frac{\alpha C_{n-1}}{\sqrt{n}} = \frac{\alpha^2 C_{n-1}}{\sqrt{(n)(n-1)}} = \frac{\alpha^n C_0}{\sqrt{n!}}, \tag{2.9}$$

here $C_0$ is a normalization constant that can be easily determined by using normalization condition

$$\sum_{n=0}^{\infty} |C_n|^2 = 1, \tag{2.10}$$

so we have

$$\sum_{n=0}^{\infty} |\frac{\alpha^n C_0}{\sqrt{n!}}|^2 = 1 \tag{2.11}$$

$$|C_0|^2 \sum_{n=0}^{\infty} \frac{|\alpha|^{2n}}{n!} = 1. \tag{2.12}$$

As we know that $e^x = \sum_{n=0}^{\infty} \frac{x^n}{n!}$ so

$$|C_0| = e^{\frac{-|\alpha|^2}{2}}, \tag{2.13}$$

so state $|\alpha\rangle$ become

$$|\alpha\rangle = e^{\frac{-|\alpha|^2}{2}} \sum_{n=0}^{\infty} \frac{\alpha^n}{\sqrt{n!}}\,|n\rangle\,. \tag{2.14}$$

Coherent state in terms of displaced vacuum state is expressed as

$$|\alpha\rangle = e^{\alpha\alpha^\dagger - \frac{-|\alpha|^2}{2}} |0\rangle = \hat{D}(\alpha) |0\rangle , \tag{2.15}$$

where $\hat{D}(\alpha)$ is a displaced vacuum operator. Here I used identity $e^{(\Omega_1+\Omega_2)} = e^{-1/2[\Omega_1,\Omega_2]} e^{[\Omega_1]} e^{[\Omega_2]}$ with fact $e^{\alpha^*\alpha} |0\rangle = |0\rangle$ so the characteristic function can be written as for coherent state

$$\chi(\zeta_1, \zeta_2) = e^{[-(\zeta_1^2+\zeta_2^2)/4 + i\zeta_1(\alpha+\alpha^*)/\sqrt{2} + i\zeta_2(\alpha-\alpha^*)/\sqrt{2}]}. \tag{2.16}$$

By comparing Eq. (2.3) and Eq. (2.6), it is concluded that coherent state is also a Guassian state.

## 2.4 One-Mode Sequeezed States

Sequeezed vacuum state refers to one mode sequeezed state, defined as

$$|\zeta, 0\rangle = S(\zeta) |0\rangle , \tag{2.17}$$

and sequeezing operator $S(\zeta)$ defined as

$$S(\zeta) = e^{(-\zeta\alpha^{\dagger 2}/2 + \zeta^*\alpha^{\dagger 2}/2)}, \tag{2.18}$$

where $\zeta = re^{i\phi}$ stand for arbitrary complex number with module r and argument $\phi$. The sequeezing operator $S(\zeta)$ is a unitary operator i.e. $S(\zeta)^\dagger = S(\zeta)^{-1}$. In order to understand characteristics of sequeezed state one can express single mode sequeezed state in terms of number state, vacuum state $|0\rangle$ satisfying a relation

$$\hat{\alpha} |0\rangle = 0. \tag{2.19}$$

Let us operate operator $S(\zeta)$ from the left and which is unitary operator, then we can write

$$S(\zeta)\hat{\alpha}S(\zeta)^\dagger S(\zeta) |0\rangle = 0, \tag{2.20}$$

or it can also written as

$$S(\zeta)\hat{\alpha}S(\zeta)^\dagger |\zeta\rangle = 0, \tag{2.21}$$

and

$$S(\zeta)\hat{\alpha}S(\zeta)^{\dagger} = \hat{\alpha}\cosh(r) + e^{i\theta}\hat{\alpha}^{\dagger}\sinh(r), \tag{2.22}$$

so the equation 1.22 can be written as

$$\hat{\alpha}\cosh(r) + e^{i\theta}\hat{\alpha}^{\dagger}\sinh(r)\,|\zeta\rangle = 0 \tag{2.23}$$

$$(\hat{\alpha}\mu + \hat{\alpha}^{\dagger}\nu)\,|\zeta\rangle = 0 \tag{2.24}$$

where $\mu = \cosh(r)$ while $\nu = e^{i\theta}\sinh(r)$. Thus (Eq. 2.24) shows squeezed vacuum state with an eigen state of $\hat{\alpha}\mu + \hat{\alpha}^{\dagger}\nu$ operator having eigen value zero. The sequeezd state, in terms of superposition of number states, is defined as

$$|\zeta\rangle = \sum_{n=0}^{\infty} C_n\,|n\rangle\,. \tag{2.25}$$

Equation (1.25) will become

$$(\hat{\alpha}\mu + \hat{\alpha}^{\dagger}\nu)\sum_{n=0}^{\infty} C_n\,|n\rangle = 0 \tag{2.26}$$

on simplificaion we get recursion relation as given blew

$$C_{n+1} = -\nu/\mu(n/n+1)^{1/2}C_{n-1} \tag{2.27}$$

There are two different solution of Eq.(2.27). One solution leads to even number of photons and second solution leads to odd number of photons. As vacuum state is related to the even solution, so here we emphasize on even case only. The solution of the recursion relation is

$$C_{2m} = (-1)^m(e^{i\theta}\tanh(r))^m[\frac{(2m-1)!!}{(2m)!!}]^{1/2}C_0, \tag{2.28}$$

$C_0$ is a normalization constant, by applying normalization condition we get

$$\sum_{m=0}^{\infty}|C_{2m}|^2 = 1, \tag{2.29}$$

so

$$(1 + \sum_{m=0}^{\infty}(\tanh(r))^{2m}[\frac{(2m-1)!!}{(2m)!!}])|C_0|^2 = 1. \tag{2.30}$$

Above relation can be simplified using an identity given below

$$(1+\sum_{m=0}^{\infty}(z)^m[\frac{(2m-1)!!}{(2m)!!}])=(1-z)^{1/2}, \tag{2.31}$$

we can write $C_0=\sqrt{\cosh(r)}$, also we know that

$$(2m)!!=2^m m! \tag{2.32}$$

$$(2m-1)!!=\frac{2m!}{2^m m!} \tag{2.33}$$

so the most common form of coefficient of single mode sequeezed vacuum state is given as

$$C_{2m}=\frac{1}{\sqrt{\cosh(r)}}(-1)^m e^{im\theta}\tanh(r))^m\frac{(2m!)^{1/2}}{2^m m!}, \tag{2.34}$$

so the single mode sequeezed state is

$$|\zeta\rangle=\frac{1}{\sqrt{\cosh(r)}}\sum_{m=0}^{\infty}(-1)^m e^{im\theta}\tanh(r))^m\frac{(2m!)^{1/2}}{2^m m!}|2m\rangle\,. \tag{2.35}$$

Above equantion showes the state for even number of photons.

## 2.5 Two Mode Sequeezed States

Thus far, we have studied non classical properties of light for single mode field. When we come across multimode field of light then non-classical effects become more prominent and different modes of field states become entangled. In this section we study two mode sequeezed state by using the analogy as we applied in single mode sequeezed vacuum state. So two mode sequeezed operator is defined as [2]

$$\hat{S}_2(\zeta)=e^{(-\zeta\hat{a}^\dagger\hat{b}^\dagger/2+\zeta^*\hat{a}^\dagger\hat{b}^\dagger/2)}, \tag{2.36}$$

where $\zeta=re^{i\phi}$ is an arbitrary complex number with sequeezing parameter r and phase $\phi$ and $\hat{a}$ and $\hat{b}$ correspond to operators for two modes with $[\hat{a}^\dagger,\hat{b}^\dagger]=0$. Further more two mode sequeezed operator can not be split into two single mode operators, so we apply it to the vacuum mode i.e $|0\rangle_a|0\rangle_b=|0,0\rangle$

$$|\zeta\rangle_2=\hat{S}_2(\zeta)|0,0\rangle \tag{2.37}$$

$$|\zeta\rangle_2 = e^{(-\zeta\hat{a}^\dagger\hat{b}^\dagger/2+\zeta^*\hat{a}^\dagger\hat{b}^\dagger/2)}\,|0,0\rangle\,. \tag{2.38}$$

$\hat{S}_2$ cannot be expressed as simple product of two single-mode squeezed operators, it implies that there exists a strong correlations between the two modes of the squeezed state. Two mode sequeezed operator consists of creation and anhilation operator for each mode of the field. Now we will try to express sequeezed state in terms of number state. For this consider the operation of anhilation operator on vacuum state i.e.

$$\hat{a}\,|0,0\rangle = 0. \tag{2.39}$$

We can write above equation as

$$\hat{S(\zeta)}_2\hat{a}\hat{S(\zeta)}_2^\dagger\hat{S(\zeta)}_2\,|0,0\rangle = 0, \tag{2.40}$$

$$\hat{S(\zeta)}_2\hat{a}\hat{S(\zeta)}_2^\dagger\,|\zeta\rangle_2 = 0, \tag{2.41}$$

and also

$$\hat{S(\zeta)}_2\hat{a}\hat{S(\zeta)}_2^\dagger\,|\zeta\rangle = \hat{a}\cosh(r) + e^{i\theta}\hat{b}^\dagger\sinh(r). \tag{2.42}$$

Equation Eq.(1.42) will become

$$\hat{a}\cosh(r) + e^{i\theta}\hat{b}^\dagger\sinh(r)\,|\zeta\rangle_2 = 0. \tag{2.43}$$

In addition we can also write

$$(\mu\hat{a} + \nu\hat{b}^\dagger)\,|\zeta\rangle_2 = 0, \tag{2.44}$$

where $\mu = \cosh(r)$ while $\nu = e^{i\theta}\sinh(r)$ now write $|\zeta\rangle_2$ as superposion of number states i.e.

$$|\zeta\rangle_2 = \sum_{n,m} C_{n,m}\,|n,m\rangle\,, \tag{2.45}$$

so Eq. (1.45) will become

$$(\mu\hat{a} + \nu\hat{b}^\dagger)\sum_{n,m} C_{n,m}\,|n,m\rangle = 0. \tag{2.46}$$

By evaluating operators above equation will become

$$\sum_{n,m} C_{n,m}[\mu\sqrt{n}\,|n-1,m\rangle + \nu\sqrt{m+1}\,|n,m+1\rangle] = 0. \tag{2.47}$$

This solution of Eq. (2.47) containing two-mode vacuum state $|0,0\rangle$ is given as

$$C_{n,m} = C_{0,0}(-\frac{\nu}{\mu})^n \delta_{n,m} = C_{0,0}(-1)^n e^{in\theta} \tanh^n(r)\delta_{n,m}, \tag{2.48}$$

where $C_{0,0}$ is a normalization constant and can be determined from normalization condition i.e. $C_{0,0} = (cosh(r))^{-1}$. Here two-mode based squeezed vacuum state expressed in form of the number states as

$$|\zeta\rangle_2 = \frac{1}{\cosh(r)} \sum_{n=0}^{\infty} (-1)^n e^{in\theta} (\tanh(r))^n |n,n\rangle . \tag{2.49}$$

Equation (2.49) showes that there is strong correlation between two modes and only paired states occur in superposition, for this reason these states are called "twin beams".

## 2.6 Covariance Matrix

N-mode Gaussian state is specified by a $2n$ dimentional covariance matrix $\gamma$ having $2n$ dimensional displacement vector d. In statistical mechanics $d$ refers to the first mean and matrix $\gamma$ refers to second mean mean of the distribution. However first moment d is adjusted arbitrary through uniform transformations and it does not effect entanglement of the system. The general form of covarient matrix $\gamma$ is defined as

$$\gamma = \begin{bmatrix} \gamma_{xx} & \gamma_{xp_x} & \gamma_{xy} & \gamma_{xp_y} \\ \gamma_{xp_x} & \gamma_{p_xp_x} & \gamma_{yp_x} & \gamma_{p_xp_y} \\ \gamma_{xy} & \gamma_{yp_x} & \gamma_{yy} & \gamma_{yp_y} \\ \gamma_{xp_y} & \gamma_{p_xp_y} & \gamma_{yp_y} & \gamma_{p_yp_y} \end{bmatrix} \tag{2.50}$$

This matrix is real, symmetric and positive. This can be be written as

$$\gamma = \begin{bmatrix} A & B \\ C^T & D \end{bmatrix} \tag{2.51}$$

Here A, B, C and D are $2 \times 2$ are hermition matrices. A and B are related to the covariance matrices to the individual one-mode state and matrix C consists on the cross corelation entries of modes.

In quantm information the first moment of any state is determind by using density

matrix formalism of that particular state as $d_j = \mathrm{Tr}(\rho R_j)$ and elements of covarient matrix is calculated by using formulla as

$$\gamma_{ij} = 2\,\mathrm{Tr}[\rho(R_j - d_j)(R_k - d_k)] - iJ_{jk} \tag{2.52}$$

Here $\hat{R} = \{\,\hat{x}, ..., \hat{x}_n, \hat{p}, ..., \hat{p}_n\,\}^T$ is a $2n$ vectors consisting on quadrature opretors and $J_{jk} = \left[\hat{R}_j, \hat{R}_k\right]$. The quadrature operators $\hat{x}$ and $\hat{p}$ defined as

$$\begin{aligned} \hat{x}_i &= \frac{\hat{a}_i^\dagger + \hat{a}_i}{\sqrt{2}} \\ \hat{p}_i &= \frac{i(\hat{a}_i^\dagger - \hat{a}_i)}{\sqrt{2}} \end{aligned} \tag{2.53}$$

We can calculate the covariance matrix of any state from its density matrix. Once we construct a density matrix then we have to make all opreations on covarience matrix alone that makes calculations much easier.

Now consider a vacuum state $|0\rangle$ with density matrix $\rho = |0\rangle\langle 0|$ the covariance matix of vacuum state is given as

$$\gamma_v = \begin{bmatrix} 1 & 0 \\ 0 & 1 \end{bmatrix} \tag{2.54}$$

Now consider a coherant state $|\alpha\rangle$ with a density matrix $\rho = |\alpha\rangle\langle\alpha|$, then covariance matrix for coherant state is identity matrix and given as

$$\gamma_c = \begin{bmatrix} 1 & 0 \\ 0 & 1 \end{bmatrix} \tag{2.55}$$

Two mode sequeezed vacuum state is given as

$$|\zeta\rangle_2 = \frac{1}{\cosh(r)} \sum_{n=0}^{\infty} (-1)^n e^{in\theta} (\tanh(r))^n \,|n, n\rangle\,. \tag{2.56}$$

Above state can be written as

$$|\psi\rangle_{SI} = \sqrt{1-\lambda^2} \sum_{n=0}^{\infty} (\lambda)^n \,|n\rangle_S \,|n\rangle_I \tag{2.57}$$

Here we have used S and I for signal and idler modes of a SPDC source. Density matrix is written as

$$\rho = 1 - \lambda^2 \sum_{n=0}^{\infty} \sum_{m=0}^{\infty} \lambda^n \lambda^{*m} \left|n\right\rangle_S \left|n\right\rangle_I \left\langle m\right|_S \left\langle m\right|_I \tag{2.58}$$

its $d$ is equal to zero and it has a $4 \times 4$ covariance matrix and it is given as

$$\gamma = \begin{bmatrix} 2\mu+1 & 2\sqrt{\mu(\mu+1)} & 0 & 0 \\ 2\sqrt{\mu(\mu+1)} & 2\mu+1 & 0 & 0 \\ 0 & 0 & 2\mu+1 & -2\sqrt{\mu(\mu+1)} \\ 0 & 0 & -2\sqrt{\mu(\mu+1)} & 2\mu+1 \end{bmatrix} \tag{2.59}$$

where $\mu = \frac{\lambda^2}{1-\lambda^2}$ and $\mu$ refers to the average no. of photons in each mode of SPDC source. Eq. (2.59) can be simplified as

$$\gamma = \begin{bmatrix} 2\mu+1 & \pm 2\sqrt{\mu(\mu+1)} \\ \pm 2\sqrt{\mu(\mu+1)} & 2\mu+1 \end{bmatrix}^{\oplus 2}, \tag{2.60}$$

where $\oplus 2$ represents direct sum.

## 2.7 Gaussian Unitary Operations

A unitary operation for a Gaussian state can be defined as an operation that acts on a Gaussian state and changes it into another Gaussian state. The Gaussain unitary operations do not destroy the Gaussian characheristics of the state. For simplicity we express a state in a form of covarience matrix and a symplectic transformation is applied on this covarience matrix and transformation is written as giedke2003entanglement.

$$\begin{aligned} \gamma &= S^T \gamma S \\ d &= S^T d \end{aligned} \tag{2.61}$$

Here $S$ represent the symplectic matrix corresponding to covarience matrix and T represents transpose of the matrix. |hlA covariance is diagonalized using symplectic transformation. The symplectic matrix is a unitary matrix i.e. $S^{-1} = S^T$. Beam splitters and phase shifts are basic elemnts of linear optics. The transformation matrix of phase shift and beam splitter is written explicity as

$$R(\phi) = \begin{bmatrix} \cos(\phi) & \sin(\phi) \\ -\sin(\phi) & \cos(\phi) \end{bmatrix}. \tag{2.62}$$

For two mode A and B ,beam splitter action is [3]

$$S_{AB}^{t} = \begin{bmatrix} \sqrt{t} & \sqrt{1-t} & 0 & 0 \\ -\sqrt{1-t} & \sqrt{t} & 0 & 0 \\ 0 & 0 & \sqrt{t} & \sqrt{1-t} \\ 0 & 0 & -\sqrt{1-t} & \sqrt{t} \end{bmatrix}. \tag{2.63}$$

Now that we have developed covariance matrix formation and symplectic form of operators. we consider varirous application of this approach in quantum information process in next chapter

# Chapter 3

# Application Of Spontaneous Paramatric Down Conversion in Quantum Information Process

In this chapter, we study Hong O Mandle Interferometer and calculate its visibility by incorporating all chanel losses. We explain EPR interferometer using two mode sequeezed vacuum state. We apply Sagnac loop in concatenated entanglement swapping and calculate visibility of the protocal by including channel losses and detector inefficiencies. In Sec. 3.1, we discuss HOM interferometer. In Sec. 3.2, we explain EPR interferometer. In Sec.3.3, we discuss concatenated entanglement swapping.

## 3.1 Hong Ou Mandle Interference from SPDC Source

Most common way to measure the duration of a short pulse of light is by superposition of two similar pulses and then we determine the overlaping by using nonlinear crystal. The other way to determine the time duration by the technique of harmonic generation in a non linear medium. However these techniques required intense beam of light and are also not favourable for more than one photon. So HOM interference is used to find time duration of two photons. When two identical photons are incident on each port of 50 : 50 beam spliter simultanously. These two photons come in one port after passing through beam splitter, no one photon follow single port. The state of emeerging

photons from beam splitter is defined as

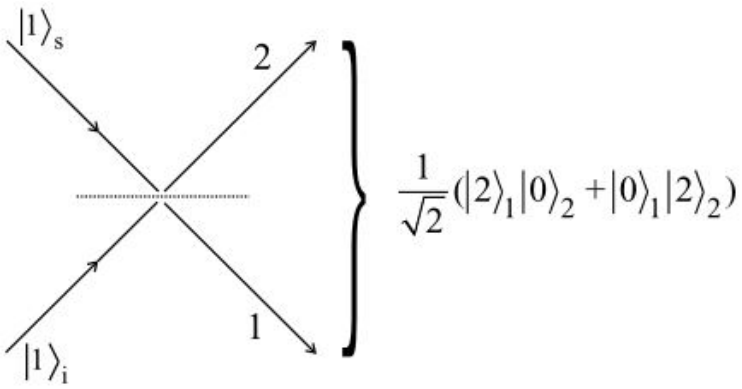


Figure 3.1: Two photons striking from SPDC source are striking and leaving the beam splitter [2].

$$|\psi_{BS}\rangle = \frac{|2\rangle_1 |0\rangle_2 + |0\rangle_1 |2\rangle_2}{\sqrt{2}}. \tag{3.1}$$

Dectecors placed at output never give simultanous count, this shows indication that photons strike on beam splitter simulanously. This fact was first explained by Hong, Ou and Mandel (HOM). HOM desigined experiment to find the time between two photons. The visibility of HOM interferometer will be equal to unity when photons have different degree of fredom, so by using this fact we can distinguish the photons in idler mode and in signal mode of the SPDC source.

The experiment of HOM interference can be described as photons from the signal and idler mode are fed to the 50 : 50 beam splitter then emerging photons are fed to the dectotors. The detectors measure the coincident count by using time dely technique. When idler beam has perfect time i.e. no time delay then graph between coincident count and beamsplitter position goes to its minimum value called HOM dip. So we can say that there is maximum overlap between signal and idler photons. The plot of HOM dip shown in Fig 3.2. The visibility of HOM is defined as

$$V_{HOM} = \frac{P^{CC}_{mean} + P^{CC}_{min}}{P^{CC}_{mean}}. \tag{3.2}$$

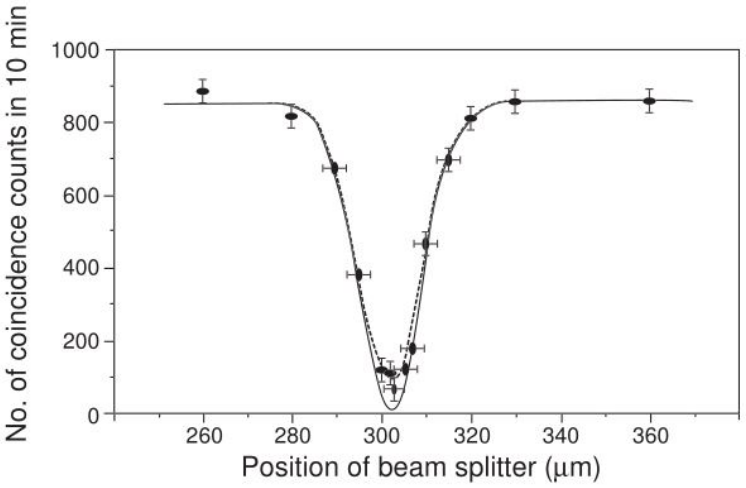


Figure 3.2: Experimental HOM effect [2]. Graph shows tha plot between concident count and position of the beam splitter, plot goes to its minimum value for perfect beam splitter position.

Here we defined $P_{min}^{CC}$ is the probability of coincidence count without delay of signal and idler mode photons while $P_{mean}^{CC}$ is the probability of coincidence count of the detectors with delay of signal and idler photons of SPDC source. When there is delay between signal and ider mode then there will be no interference and graph is wider.
In order to determine the acceptance of HOM interference that is discuss in where the visisbility of HOM interference depend upon the pump power which is determined experimently with standard mode-locked laser (Ti:Sapphire laser of frequency 76 MHz). The experiment setup and theoretical model shown in Fig 3.3.

As working mathematically, we use Two Mode Sequeezed Vacuum (TMSV) state as a state of SPDC source. TMSV state have all muliphoton effects in it. As we know that when signals are propagate then signals come under the environmental effects that cause the signal losses in signal mode (A) and in idler mode (B). These transmission losses are described in term of transmittance $t_{A,B}$ of beam splitters respectivily. $t_B$ also contain the losses of controllable delay line that is described by the collimator in experimental setup, this makes setup asymmetric i.e. $t_A \neq tB$. How detectors determine the photon and give clicks is called the efficiency of the detectors. Here in

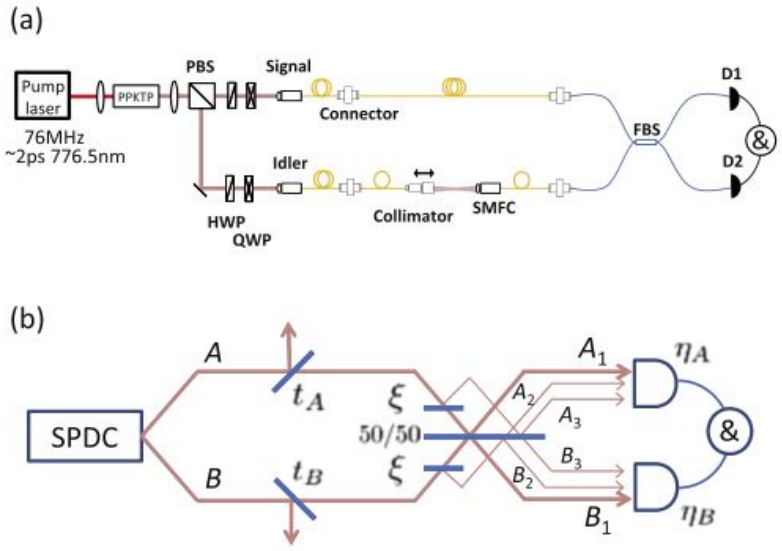


Figure 3.3: (a) gives experimental arraengement of HOM intereferance experiment and (b) give a theoritical model of HOM interference experiment [3].

theoretical model we show the efficiency of detectors by $\eta_a$ and $\eta_b$ respectivily for two detectors. The mode mismatch of signal and idler mode at beam splitter is defined by $\zeta$.

The covariance matrix of the TMSV state is describe in Eq.(2.59) is $\gamma_{AB}^{TMSV}$. If $t_A$ and $t_B$ is the transmittance then corresponding losses in modes can be modeled as.

$$\gamma_{AB}^{L} = L_B^{t_B} L_A^{t_A} \gamma_{AB}^{TMSV}(\mu) \tag{3.3}$$

where $L_A^{t_A}$ $L_B^{t_B}$ are losses in mode A and B respectivily. It can also be written as

$$\gamma_{AB}^{L} = \kappa_{AB}^{t_A t_B} \gamma_{AB}^{TMSV}(\mu) \kappa_{AB}^{t_A t_B} + \alpha_{AB}^{t_A t_B} \tag{3.4}$$

here we defined

$$\kappa_{AB}^{t_A t_B} = \begin{bmatrix} \sqrt{t_A} & 0 \\ 0 & \sqrt{t_B} \end{bmatrix}, \tag{3.5}$$

and

$$\alpha_{AB}^{t_A t_B} = \begin{bmatrix} 1 - t_A & 0 \\ 0 & 1 - t_B \end{bmatrix}. \tag{3.6}$$

Where $\kappa_{AB}^{t_A t_B}$ is a transmission matrix of mode A and B and $\alpha_{AB}^{t_A t_B}$ is a absorption matrix of mode A and B in lossy channel through propagation. Now after simplifications of Eq. (3.4) we get

$$\gamma = \begin{bmatrix} 2t_A\mu + 1 & \pm 2\sqrt{t_A t_B \mu(\mu+1)} \\ \pm 2\sqrt{t_A t_B \mu(\mu+1)} & 2t_B\mu + 1 \end{bmatrix}^{\otimes 2}. \tag{3.7}$$

Now theoretically application of $50:50$ beam splitter is defined on each mode as

$$\gamma^{BS}_{A_1A_2A_3B_1B_2B_3} = S^T_{BS} S_{MM} (\gamma^L_{A_1B_1} \otimes I_{A_2B_2A_3B_3}) S_{MM} S_{BS}. \tag{3.8}$$

The mode mismatch is introduced by the beam splitter and it it is cdefined as

$$S_{MM} = S^{\zeta}_{B_1B_2} S^{\zeta}_{A_1A_2}, \tag{3.9}$$

and

$$S_{BS} = S^t_{A_3B_3} S^t_{A_2B_2} S^t_{A_1B_1}. \tag{3.10}$$

For $50:50$ beam splitter transmittance is $\frac{1}{2}$ and $I_{A_2B_2A_3B_3}$ is an $8 \times 8$ identity matrix showing vacuum in mode $A_2A_3B_2B_3$. As photons propagate through a lossy channel so the covariance matrix after applying the channel losses $\eta_a$ and $\eta_b$ can be written as

$$\gamma_{A1,\ldots,B3} = L^{\eta_b}_{B_1B_2B_3} L^{\eta_a}_{A_1A_2A_3} \gamma^{BS}_{A_1,\ldots,B_3} \tag{3.11}$$

Now coincidence count probability can be calculated as

$$P^{CC}_{min} = \mathrm{Tr}\left[\hat{\rho}^{\gamma_{A_1,\ldots,B_3}} \left(\hat{I} - |0\rangle\langle 0|^{\otimes 3}\right)_{A_1A_2A_3} \left(\hat{I} - |0\rangle\langle 0|^{\otimes 3}\right)_{B_1B_2B_3}\right]$$

$$= 1 - \mathrm{Tr}\left[\hat{\rho}^{\gamma_{A_1A_2A_3}} |0\rangle\langle 0|^{\otimes 3}_{A_1A_2A_3}\right] - \mathrm{Tr}\left[\hat{\rho}^{\gamma_{B_1B_2B_3}} |0\rangle\langle 0|^{\otimes 3}_{B_1B_2B_3}\right] - Tr\left[\hat{\rho}^{\gamma_{A_1,..,B_3}} |0\rangle\langle 0|^{\otimes 6}_{A_1,\ldots,B_3}\right] \tag{3.12}$$

$$= 1 - \frac{8}{\sqrt{\det\left(\gamma_{A_1A_2A_3} + \hat{I}\right)}} - \frac{8}{\sqrt{\det\left(\gamma_{B_1B_2B_3} + \hat{I}\right)}} - \frac{64}{\sqrt{\det\left(\gamma_{A_1,\ldots,B_3} + \hat{I}\right)}} \tag{3.13}$$

Here we used formula

$$Tr\left[\hat{\rho}^{\gamma} |0\rangle\langle 0|^{\otimes m}\right] = \frac{2^m}{\sqrt{det(\gamma + \hat{I})}} \tag{3.14}$$

and $\gamma_{A_1}\gamma_{A_2}\gamma_{A_3}$ and $\gamma_{B_1}\gamma_{B_2}\gamma_{B_3}$ are submatrics of $\gamma_{A_1}, ..., \gamma_{B_3}$. Now we will evaluate the terms of Eq.(3.13) as fellow

$$\sqrt{\det\Big(\gamma_{A_1A_2A_3}+\hat{I}\Big)} = 8\Bigg\{\Bigg[1+\frac{\eta_a\mu}{4}\Bigg\{2(t_a-t_b)-t_at_b\eta_a(1-\zeta^2)\Bigg\}\Bigg]^2 - t_at_b\zeta^2\eta_a^2\mu(\mu+1)\Bigg\}^{\frac{1}{2}} \tag{3.15}$$

$$\sqrt{\det\Big(\gamma_{B_1B_2B_3}+\hat{I}\Big)} = 8\Bigg\{\Bigg[1+\frac{\eta_b\mu}{4}\Bigg\{2(t_a-t_b)-t_at_b\eta_a(1-\zeta^2)\Bigg\}\Bigg]^2 - t_at_b\zeta^2\eta_b^2\mu(\mu+1)\Bigg\}^{\frac{1}{2}} \tag{3.16}$$

$$\begin{aligned}\sqrt{det(\gamma_{A_1\ldots B_3}+\hat{I})} = 64\Bigg[\Bigg\{1+\frac{\mu}{4}\Bigg[2(t_a-t_b)(\eta_a+\eta_b) \\ -t_at_b\Big\{(\eta_a+\eta_b)^2-\zeta^2(\eta_a-\eta_b)^2\Big\}\Bigg]\Bigg\}^2 - t_at_b(\eta_a-\eta_b)^2\zeta^2\mu(\mu+1)\Bigg]^{\frac{1}{2}}\end{aligned} \tag{3.17}$$

When we set $\zeta = 0$ in $P^C_{min}C$ then we get coincidence count for decay choice i.e. $P^{CC}_{mean}$ Now if $\eta_a = \eta_b = \eta \ll 1$ and $t_a = t_b = \zeta = 1$ and with assumption that $\mu \ll 1$ then we can easily find visibility of HOM interferometer.

$$V_{HOM} \approx \frac{1+2\mu}{1+4\mu} \approx 1-2\mu. \tag{3.18}$$

For most suitable condition i.e. $t_A = t_B = \eta_A = \eta_B = \zeta = 1$ and $\mu \ll 1$ then we have

$$V_{HOM} \approx \frac{2+2\mu}{2+3\mu} \approx 1-\frac{1}{2}\mu. \tag{3.19}$$

Above relation defines visibility degrades due emission of many photons that go on inceasing due to inefficiency of detectors.

## 3.2 EPR Interference of a Sagnac loop Entanglement Source

The EPR interference experiment is most commonly used and comparativilty an easier way to determine the entanglement between two pairs experimently. In this test each spatial mode of the photon beam having a specific polarization strikes on a half wave plate (HWP) then subjected to the polarization beam splitter (PBS). When photons

stike on the polarization beam splitter then photons get a particular polarization and is then fed to a single photon detector. When we change the angle of polarization for each polarization of photons then we get different coincidence count rate. It means that coincidence count rate depends upon the angle of polarizatrion. Interenference fringes are obtained if we fix one angle and shuffle the values of second angle. The visibilty for EPR interference can be defined as

$$V_{ent} = \frac{P_{max}^{CC} - P_{min}^{CC}}{P_{max}^{CC} + P_{min}^{CC}}, \tag{3.20}$$

here $P_{max}^{CC}$ and $P_{min}^{CC}$ stands for maximum and minimum count rate of interference fringes. The experimental setup and corresponding linear model for EPR interference is given in Fig 3.4. The Sagnace loop produces two mode sequeezed vacuum (TMSV) state. The polarizarion mode travel in clockwise direction and in theoretical model it is represented by $A_H$ and $A_V$ while the polarization modes that travel in anti-clockwise direction and it is represted by $B_H$ and $B_V$ in theoretical model. We can generate the entangled state using dichoric polarization beam splitter, which switches vertical polarization of $A_V$ and $B_V$ modes.

For two, two-mode sequeezed vacuum state covariance matrix given below

$$\gamma_{A_H A_V B_H B_V}^{TMSV2} = \begin{bmatrix} 2\mu+1 & \pm 2\sqrt{\mu(\mu+1)} & 0 & 0 \\ \pm 2\sqrt{\mu(\mu+1)} & 2\mu+1 & 0 & 0 \\ 0 & 0 & 2\mu+1 & \pm 2\sqrt{\mu(\mu+1)} \\ 0 & 0 & \pm 2\sqrt{\mu(\mu+1)} & 2\mu+1 \end{bmatrix}^{\oplus 2} \tag{3.21}$$

When the covarience matrix $\gamma_{A_H A_V B_H B_V}^{TMSV2}$ passes through the sagnac loop then we will get $\gamma_{A_H A_V B_H B_V}^{SL}$ as

$$\gamma_{A_H A_V B_H B_V}^{TMSV2} = \begin{bmatrix} 2\mu+1 & 0 & 0 & \pm 2\sqrt{\mu(\mu+1)} \\ 0 & \pm 2\sqrt{\mu(\mu+1)} & 2\mu+1 & 0 \\ 0 & 2\mu+1 & \pm 2\sqrt{\mu(\mu+1)} & 0 \\ \pm 2\sqrt{\mu(\mu+1)} & 0 & 0 & 2\mu+1 \end{bmatrix}^{\oplus 2}. \tag{3.22}$$

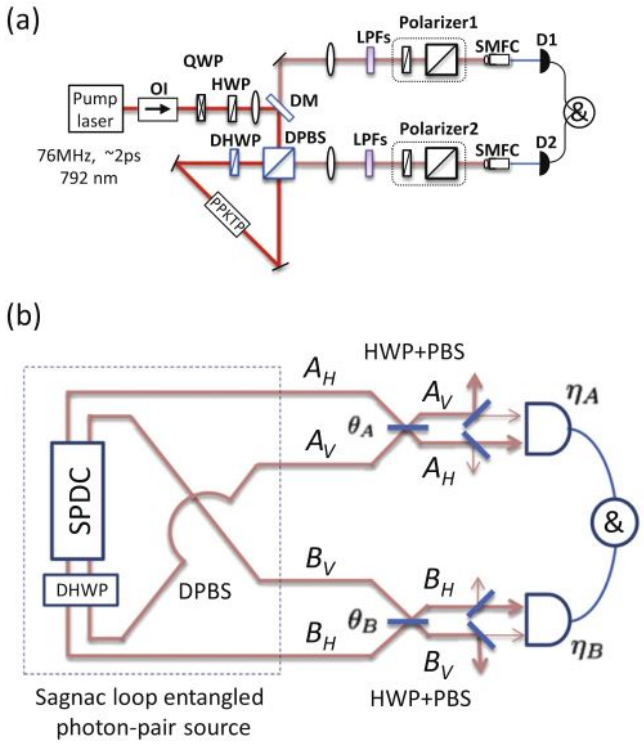


Figure 3.4: (a) Experimental set up for EPR interference, and (b) corresponding linear optical model [3]. linear model contains non liear crystal PPKTP, optical iscolator (OI), dichoric mirror(DM), quarter waveplate (QWP), dichroic half waveplate (DHWP) dichroic polarization beamsplitter (DBPS), single-modefiber coupler (SMFC), long wavelength pass filter(LPF) [3].

HWP and PBS jointly work as a beam splitter of transmittance $\cos^2\theta$ between horizontal and vertical compnents of polarization. The calculations of theoretical models can be simplified by using $\tilde{\eta_H} = t_H\eta_H$ and $\tilde{\eta_V} = t_V\eta_V$ here $\eta_H$ and $\eta_V$ stands for efficiences of detectors. First of all we apply the beam splitter action $S^{\theta_A}_{A_HA_V}S^{\theta_A}_{A_HA_V}$ on the horizontal and vertical components of covariance matrix. Here we incorporate all imperfections of detectors and polarization beam splitter in lossy channel as $L^{\eta\tilde{B_V}}_{B_V}L^{\eta\tilde{B_H}}_{B_H}L^{\eta\tilde{A_V}}_{A_V}L^{\eta\tilde{A_H}}_{A_H}$. The coincidence count probability can be calculated as

$$P^{CC}_{\theta_A\theta_B} = Tr\left[\hat{\rho}^{\gamma_{A_HA_VB_HB_V}}\left(\hat{I} - |0\rangle\langle 0|^{\otimes 2}\right)_{A_HA_V}\left(\hat{I} - |0\rangle\langle 0|^{\otimes 2}\right)_{B_HB_V}\right]. \tag{3.23}$$

$$= 1 - \frac{4}{\sqrt{det(\gamma_{A_H A_V} + \hat{I})}} - \frac{4}{\sqrt{det(\gamma_{B_H B_V} + \hat{I})}} + \frac{16}{\sqrt{det(\gamma_{A_H A_V B_H B_V} + \hat{I})}} \tag{3.24}$$

Here we can solve above equation as

$$\sqrt{det(\gamma_{A_H A_V} + \hat{I})} = \sqrt{\left(2 - \tilde{\eta}_{A_H} + \tilde{\eta}_{A_H}\left((2\mu+1)\cos^2\theta_A + (2\mu+1)\sin^2\theta_A\right)\right)^2} \tag{3.25}$$

$$\sqrt{\left(2 - \tilde{\eta}_{A_V} + \tilde{\eta}_{A_V}\left((2\mu+1)\cos^2\theta_A + (2\mu+1)\sin^2\theta_A\right)\right)^2} \tag{3.26}$$

$$\sqrt{det(\gamma_{A_H A_V} + \hat{I})} = \sqrt{16\left(1 + \tilde{\eta}_{A_H}\mu\right)^2\left(1 + \tilde{\eta}_{A_V}\mu\right)^2} \tag{3.27}$$

$$= \sqrt{det(\gamma_{A_H A_V} + \hat{I})} = 4\left(1 + \tilde{\eta}_{A_H}\mu\right)\left(1 + \tilde{\eta}_{A_V}\mu\right) \tag{3.28}$$

$$\sqrt{det(\gamma_{B_H B_V} + \hat{I})} = \sqrt{\left(2 - \tilde{\eta}_{B_H} + \tilde{\eta}_{B_H}\left((2\mu+1)\cos^2\theta_B + (2\mu+1)\sin^2\theta_B\right)\right)^2}$$
$$\sqrt{\left(2 - \tilde{\eta}_{B_V} + \tilde{\eta}_{B_V}\left((2\mu+1)\cos^2\theta_B + (2\mu+1)\sin^2\theta_B\right)\right)^2} \tag{3.29}$$

$$\sqrt{det(\gamma_{B_H B_V} + \hat{I})} = \sqrt{16\left(1 + \tilde{\eta}_{B_H}\mu\right)^2\left(1 + \tilde{\eta}_{B_V}\mu\right)^2} \tag{3.30}$$

$$\sqrt{det(\gamma_{B_H B_V} + \hat{I})} = 4\left(1 + \tilde{\eta}_{B_H}\mu\right)\left(1 + \tilde{\eta}_{B_V}\mu\right) \tag{3.31}$$

$$\sqrt{det(\gamma_{A_H A_V B_H B_V} + \hat{I})} = 8\Bigg[\left\{1 + \left(\tilde{\eta}_{A_H} + \tilde{\eta}_{B_H} - \tilde{\eta}_{A_H}\tilde{\eta}_{B_H}\right)\mu\right\}\left\{1 + \left(\tilde{\eta}_{A_V} + \tilde{\eta}_{B_V} - \tilde{\eta}_{A_V}\tilde{\eta}_{B_V}\right)\mu\right\}$$
$$+\left\{1 + \left(\tilde{\eta}_{A_H} + \tilde{\eta}_{B_V} - \tilde{\eta}_{A_H}\tilde{\eta}_{B_V}\right)\mu\right\}\left\{1 + \left(\tilde{\eta}_{A_V} + \tilde{\eta}_{B_H} - \tilde{\eta}_{A_V}\tilde{\eta}_{B_H}\right)\mu\right\}$$
$$\left(\tilde{\eta}_{A_H} - \tilde{\eta}_{A_V}\right)\left(\tilde{\eta}_{B_H} - \tilde{\eta}_{B_V}\right)\mu(\mu+1)\cos 2\left(\theta_A + \theta_B\right)\Bigg] \tag{3.32}$$

The coincidence count for minimun probability $P_{min}^{CC}$ are calculated by putting $\theta_A = 0$ and $\theta_B = 0$ and maximum probability $P_{max}^{CC}$ is calulate by putting and one ange equal

to $\frac{\pi}{2}$ The calculation can be simplified by using $\tilde{\eta}_{A_H} = \tilde{\eta}_{B_H} = \eta$ and $\tilde{\eta}_{A_H} = \tilde{\eta}_{B_H} = 0$, so visibility is

$$V_{ent} = \frac{1+\mu}{1+3\mu+2\eta(2-\eta)\mu^2} \tag{3.33}$$

Now in case of weak pumping $\mu \ll 0$ then we get

$$V_{ent} \approx 1 - 2\mu. \tag{3.34}$$

Which shows visibility depends linearily upon $\mu$.

## 3.3 Concatenated Entanglement Swapping

As in quantum communication when photons are used for a source of signal transfer, then photons come under the environmental effects and this limits the long distance communications. Dark counts also make things more complicated when detectors clicks even in the absence of photons, so due to loss of original photon and dark count limit the communcations upto 200 km. One solution of this problem is a quantum repeaters. In quantum repeaters we use memories at different positions along a path to retrieve a lost information. Still a lot of work is needed in the field of quantum repeaters and it become difficult with current technologies. Concatenating entanglement swapping is a better way to work with current technologies to extend the distance of communication. Setup of concatenated entanglement swapping is called quantum relay. In cancatenated entantaglment swapping two pariticles that are for away from each other get entangled by a process of entanlement swapping between particles. This proecss enhances the entaglement between particals and increases the communication distance between two parties.

Here we use a protocal simmiler to protocal that is dicsuss in [14], where state vector formuaism is used. A two- mode based sequeezed vacuum state generated from the SPDC source is used and density matrix is calculated step by step expilicity and then visibilty from the detection probabilities of the EPR interfernce. Schematic of concatenated entanglement swapping is shown in Fig 3.5.

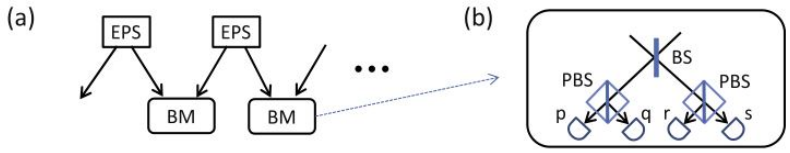


Figure 3.5: Schematic of concatenated entanglement swapping [3].

Entangled photons are generated from EPR source. The photons from EPR source come under the joint Bell measuremnt that swaps the entanglement between different modes of the beam. The Bell measurement consists on 50 : 50 beam splitter, two polarization beam splitters and four detectors as shown in Fig 3.5 (b). After passing from the beam splitter the beam comes at polarization beam splitter, the polarization beam splitter sends the photons in a particular polarization to a detector that gives clicks. Bell Measurement will be sucessful if any two detectors will gives clicks.

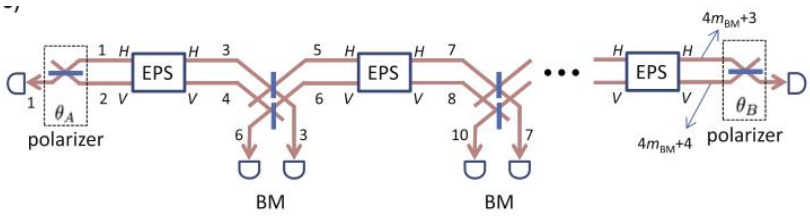


Figure 3.6: A linear optical model for concatenated entanglement swapping [3]

Fig. (3.6) shows linear setup for concatenated entanglement swapping. We review covariance matrix formalism, which is used in [3] . In linear setup Sagnac loop is used as an entangled photon source and horizontal and vertical modes of polarization are mentioned here just by lines. To overcome the sysytem imperfection we use assumptions that channel is lossy, detectors have dark counts , beam splitter and polarization beam splitter are taken as perfect. Fig. (3.6) is labled from left to right with polarization modes. Only two detectors instead of four are shown in Fig. (3.6) that gives clicks for sucessful Bell measurement. Visibility is measured by two polarizers placed at the end of the protocol. Joint detection probability is calculated including all detectors as function of polarizer angles $\theta_A$ and $\theta_B$. By seeing the linear optical model, it is found

that if there are $m_{BM}$ Bell measurements then there should be $m_{BM}+1$ Sagnac loop sources in a protocol. So the covariance matrix is $\gamma^{SL\oplus(m_{BM}+1)}$ and it can also written as

$$\begin{bmatrix} \gamma_{\pm}^{SL}(\mu) & 0 & ... \\ 0 & \gamma_{\pm}^{SL}(\mu) & \\ \vdots & & \ddots \end{bmatrix}^{\oplus 2} \tag{3.35}$$

Here we have defined $\gamma^{SL} = \left(\gamma_{\pm}^{SL}(\mu)\right)^{\oplus 2}$ and $\gamma_{\pm}^{SL}(\mu)$ show the components of the two quadratures and also we assume that all channel losses and detectors are identical. So we will apply beam splitter action to the channel first. The beam splitter action mixes mode $4x-1$ and $4x+1$ for horizontal polarization and it mixes $4x$ and $4x+2$ for vetical polarization modes here $x = 1, 2, 3, ...m_{BM}$, So symplectric matrix can be applied as

$$S_BM = \prod_{n=1}^{m_{BM}} S_{4x-1,4x+1}^{1/2} S_{4x,4x+2}^{1/2} \tag{3.36}$$

The two Polarizers at the end of the concatenated process can be applied as

$$S_{A,B} = S_{1,2}^{\theta_A} S_{4m_{BM}+3,4m_{BM}+4}^{\theta_B} \tag{3.37}$$

If $\eta$ is the efficiency of the detectors the it can be applied to the whole system as

$$L_{tot}^{\eta} = L_{4m_{BM}+4}^{\eta} ... L_1^{\eta} \tag{3.38}$$

the total covarience matrix can be obtained as

$$\gamma_{m_{BM}}^{CES} = L_{tot}^{\eta}\left(S_{AB}^T S_{MB}^T \gamma^{SL\oplus(m_{BM}+1)} S_{BM} S_{AB}\right) \tag{3.39}$$

The joint detection probability of the sysytem can be calculated as

$$\begin{aligned} P_{\theta_A,\theta_B}^{CES} &= Tr\Bigg[\hat{\rho}^{\gamma_{m_{BM}}^{CES}} \left(\hat{I} - (1-\nu)\left|0\right\rangle\left\langle 0\right|\right)_1 \left(\hat{I} - (1-\nu)\left|0\right\rangle\left\langle 0\right|\right)_{4m_{BM}+3} \\ &\times \prod_{n=1}^{m_{BM}} \left(\hat{I} - (1-\nu)\left|0\right\rangle\left\langle 0\right|\right)_{4m_{BM}+1} \left(\hat{I} - (1-\nu)\left|0\right\rangle\left\langle 0\right|\right)_{4m_{BM}+2}\Bigg] \end{aligned} \tag{3.40}$$

$$= 1 + \sum_{m=1}^{M} \sum_{C(M,m)}^{{}^{M}C_m} \frac{\{-2(1-\nu)\}^m}{\sqrt{det\left(\gamma_{C(M,m)}^{CES}\right) + \hat{I}}} \tag{3.41}$$

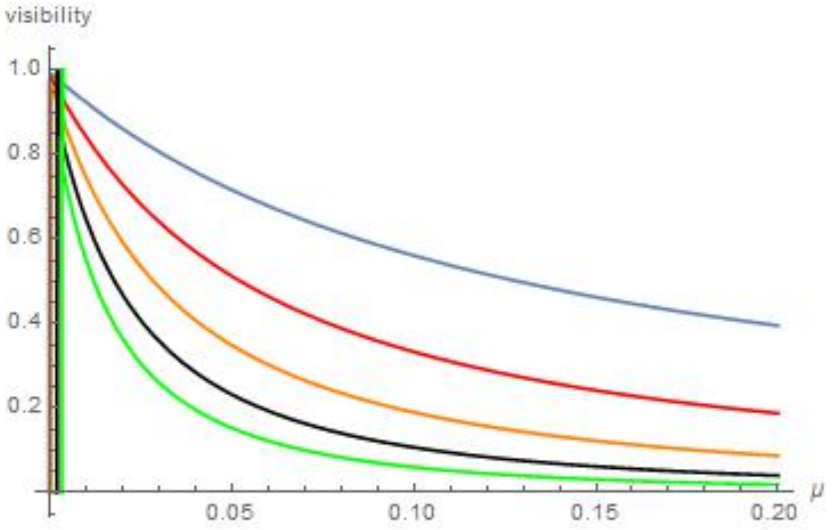


Figure 3.7: The plot shows the EPR interference visibilities for different number of concatenations as a function of average no. of photons with $\eta = .04$ and $\nu = 10^{-5}$. The blue, red, orange, black and green line represesnts Bell measurements 1, 2, 3, 4, 5 respectivily

here $\nu$ give dark count probability of the detectors and number of clicking dectors are shown by M and $M = 2m_{BM} + 2$ and $\gamma^{CES}_{C(M,m)}$) corresponds to the submatrix of $\gamma^{CES}$ with mode $C$(M,m). $C$(M,m) stands the combination cliked detectors. Now if we have $m_{BM} = 1$ then its means that there is only one Bell measurement, then total number of detectors clicking will be four and will be placed at positions 1, 3, 6, 7. It can be written with different combinations as $C(4,1) = 1, 3, 6, 7$ , $C(4,2) = 13, 16, 17, 36, 37, 67$ $C(4,3) = 136, 137, 167, 367$ and $C(4,4) = 1367$

I have generated these plots of visibilities from a general mathematica program. I have developed a general program on mathematica for any number of concatenation. My program is very efficient than previous ones. Program is very flexible, it just require number of Bell measurement of concatenated sysytem and can plot visibility graphs upto 5 bell measurements in few minutes with the help of commercially available computers. This includes covariance matrix of a Guassian state and follow the general beam splitter transformation. These interference visibilities are ploted as a function

of average photon number $\mu$ for Bell measurement $1, 2, ..., 5$ with parameters transmittance of channel $\eta = .04$ and dark count of the channel is $\nu = 10^{-15}$. The plots for $1, 2, ..., 5$ are shown in Fig. 3.7. For $m_{BM} = 1$ the graph is represented by a blue line that becomes parallel to x-axis and it shows poor distribution of entanglement due to over lapping of photons. For $m_{BM} = 2$ the graph is represented by red line, visibility is increased but not significantly it just goes up to 0.2 and then becomes parallel to x-axis and $\mu$ is also very small in this region. For $m_{BM} = 5$ the visibility graph is representd by green line, visibility increases with minimum number of photons and then graph decrease sharply with a small increase in number of photons. For $m_{BM} = 3, 4$ visibilty graph is represented by orange and black line respectivily, this shows an optimum conditions for cancatenating entanglement swapping. So from the above calculations it is clear that for practical concatenating entanglement swapping we have to select number of cancatenation carefully depending upon distance and detector parameters.

This method is efficient and well ordered method to determine the feasibility of concatenating entanglement swapping in long distance practical applications. Here we take total transmittance including efficiency of detectors $\eta_D$ and transmission of channel as $\eta = \eta_D \times 10^{\frac{\alpha L}{10}}$ $\alpha$ is loss co-efficient and L stands for transmission length. In above discussion we assume the photon pair at 1500 nm and standard optical fiber of $\alpha = 0.2$ for tansmission channel. For vaer larg $N$ this method becomes insignificant . For large number of $N$ the calculation complexity grows exponencially. This is clearly seen because in first step we have to calculate the covarience matrix of the given state including losses and beam splitter, this step includes multiplications of square matrices and matrics are polynomials order of $(O(N^3))$. In second step we have to find determinents of each sub matrix mentioned in the formula of visibility. When terms in second line of visibiliy are increased as $2^N$ and first line include the $N$ multiplication of binomial terms $(1 - \nu) |0\rangle \langle 0|$), hence it makes this method inefficient in simulation of large number of networks.

# Chapter 4

# Conclusion

In this thesis we review some quantum information process using Gaussian states and and linear optical operations [3]. We start with a Guassian state that are closely related to the laser light. We try to write characteristic function of all states and then we construct covariance matrix from this state. With covarience matrix, beam splitter and polarizer we calculate interference visibilities for concatenated entanglement swapping protocol upto five Bell measurement. We have developed a general mathematica program to calculate visibilities.

In this process all multiphoton effects and channel imperfections are incorporated, it will be proven handy to determine the performance of various experiments. Time saving is a big advantage of this approach over a state vector approach. This technique is also useful application in multi-partite entanglement generation, quantum key distribution and quantum repeater with SPDC sources. Finally as system becoms big, it contains more number of measurements and calculatons become complex. This is mentioned earlier that complexity grows as of order of $(O(N^3))$ and with current technologies it become impossible to simulate large systems. It is difficult to simulate big systems as it works with linear optics with ideal single photon and photon resolution detector, which is why linear optics with feedback are incorporated into universal computers. The covariance matrix is faster to compute than state vector approach, yet it also have some limitations and cannot be used for very large $N$.

# Appendices

## 4.0.1 Appendix A

The calulations are appended below:

$$\sqrt{det(\gamma_{A_H A_V B_H B_V} + \hat{I})} = \sqrt{\tilde{\eta}_{A_V}}\sqrt{\tilde{\eta}_{B_V}}\Big(-2\sqrt{\mu(1+\mu)}\cos\theta_B\sin\theta_A - 2\sqrt{\mu(1+\mu)}\cos\theta_A\sin\theta_B\Big)$$
$$\Big(-\sqrt{\tilde{\eta}_{A_V}}\sqrt{\tilde{\eta}_{B_V}}(2-\sqrt{\tilde{\eta}_{A_H}}\sqrt{\tilde{\eta}_{A_H}}((1+2\mu)\cos^2\theta_A+(1+2\mu)\sin^2\theta_A))\Big)\sqrt{\tilde{\eta}_{A_V}}\sqrt{\tilde{\eta}_{B_V}}\Big(-$$
$$2\sqrt{\mu(1+\mu)}\cos\theta_B\sin\theta_A - 2\sqrt{\mu(1+\mu)}\cos\theta_A\sin\theta_B\Big)(2-\sqrt{\tilde{\eta}_{B_H}}\sqrt{\tilde{\eta}_{B_H}}((1+2\mu)\cos^2\theta_B$$
$$+(1+2\mu\sin^2\theta_B))\sqrt{\tilde{\eta}_{A_V}}\sqrt{\tilde{\eta}_{B_V}}\Big(2\sqrt{\mu(1+\mu)}\cos\theta_B\sin\theta_A + 2\sqrt{\mu(1+\mu)}\cos\theta_A\sin\theta_B\Big)$$
$$\Big(\sqrt{\tilde{\eta}_{A_H}}\sqrt{\tilde{\eta}_{B_H}}\Big(-2\sqrt{\mu(1+\mu)}\cos\theta_B\sin\theta_A - 2\sqrt{\mu(1+\mu)}\cos\theta_A\sin\theta_B\Big)\Big(\sqrt{\tilde{\eta}_{A_V}}\sqrt{\tilde{\eta}_{A_H}}\sqrt{\tilde{\eta}_{B_V}}$$
$$\sqrt{\tilde{\eta}_{B_H}}\Big(2\sqrt{\mu(1+\mu)}\cos\theta_B\sin\theta_A + 2\sqrt{\mu(1+\mu)}\cos\theta_A\sin\theta_B\Big)\Big(2\sqrt{\mu(1+\mu)}\cos\theta_B\sin\theta_A +$$
$$2\sqrt{\mu(1+\mu)}\cos\theta_A\sin\theta_B\Big) - \sqrt{\tilde{\eta}_{A_V}}\sqrt{\tilde{\eta}_{A_H}}\sqrt{\tilde{\eta}_{B_V}}\sqrt{\tilde{\eta}_{B_H}}\Big(2\sqrt{\mu(1+\mu)}\cos\theta_B\sin\theta_A + 2\sqrt{\mu(1+\mu)}$$
$$\cos\theta_A\sin\theta_B\Big)^2\Big) - \Big(\sqrt{\tilde{\eta}_{A_V}}\sqrt{\tilde{\eta}_{B_V}}(2-\sqrt{\tilde{\eta}_{A_H}}\sqrt{\tilde{\eta}_{A_H}}((1+2\mu)\cos^2\theta_A+(1+2\mu)\sin^2\theta_A))\Big)\sqrt{\tilde{\eta}_{A_V}}\sqrt{\tilde{\eta}_{B_V}}$$
$$\Big(2\sqrt{\mu(1+\mu)}\cos\theta_B\sin\theta_A+2\sqrt{\mu(1+\mu)}\cos\theta_A\sin\theta_B\Big)(2-\sqrt{\tilde{\eta}_{B_H}}\sqrt{\tilde{\eta}_{B_H}}((1+2\mu)\cos^2\theta_B+$$
$$(1+2\mu)\sin^2\theta_B))\Big) - \sqrt{\tilde{\eta}_{A_H}}\sqrt{\tilde{\eta}_{B_V}}\Big(2\sqrt{\mu(1+\mu)}\cos\theta_A\cos\theta_B - 2\sqrt{\mu(1+\mu)}\sin\theta_A\sin\theta_B\Big)$$
$$\Big(\sqrt{\tilde{\eta}_{A_V}}\sqrt{\tilde{\eta}_{B_H}}\Big(2\sqrt{\mu(1+\mu)}\cos\theta_A\cos\theta_B - 2\sqrt{\mu(1+\mu)}\sin\theta_A\sin\theta_B\Big)\Big(\sqrt{\tilde{\eta}_{A_V}}\sqrt{\tilde{\eta}_{A_H}}\sqrt{\tilde{\eta}_{B_V}}\sqrt{\tilde{\eta}_{B_H}}$$
$$\Big(2\sqrt{\mu(1+\mu)}\cos\theta_B\sin\theta_A+2\sqrt{\mu(1+\mu)}\cos\theta_A\sin\theta_B\Big)\Big(2\sqrt{\mu(1+\mu)}\cos\theta_B\sin\theta_A+2\sqrt{\mu(1+\mu)}$$
$$\cos\theta_A\sin\theta_B\Big)\Big(2\sqrt{\mu(1+\mu)}\cos\theta_B\sin\theta_A+2\sqrt{\mu(1+\mu)}\cos\theta_A\sin\theta_B\Big) - \sqrt{\tilde{\eta}_{A_V}}\sqrt{\tilde{\eta}_{A_H}}\sqrt{\tilde{\eta}_{B_V}}\sqrt{\tilde{\eta}_{B_H}}$$
$$\Big(2\sqrt{\mu(1+\mu)}\cos\theta_A\cos\theta_B+2\sqrt{\mu(1+\mu)}\sin\theta_A\sin\theta_B\Big)^2\Big) + \sqrt{\tilde{\eta}_{A_H}}\sqrt{\tilde{\eta}_{B_V}}(2-\sqrt{\tilde{\eta}_{A_V}}\sqrt{\tilde{\eta}_{A_V}}((1+$$
$$2\mu)\cos^2\theta_A+(1+2\mu)\sin^2\theta_A))\Big(2\sqrt{\mu(1+\mu)}\cos\theta_A\cos\theta_B - 2\sqrt{\mu(1+\mu)}\sin\theta_A\sin\theta_B\Big)(2-$$
$$\tilde{\eta}_{B_H}\tilde{\eta}_{B_H}((1+2\mu)\cos^2\theta_B + (1+2\mu)\sin^2\theta_B))\Big) + (2-\tilde{\eta}_{B_V}\tilde{\eta}_{B_V}((1+2\mu)\cos^2\theta_B + (1+$$
$$2\mu)\sin^2\theta_B))\Big(-\tilde{\eta}_{A_V}\tilde{\eta}_{B_H}(2-\tilde{\eta}_{A_H}\tilde{\eta}_{A_H}((1+2\mu)\cos^2\theta_A+(1+2\mu)\sin^2\theta_A))\Big(2\sqrt{\mu(1+\mu)}\cos\theta_A\cos\theta_B$$

$$-2\sqrt{\mu(1+\mu)}\sin\theta_A\sin\theta_B\Big)^2+(2-\tilde{\eta}_{A_V}\tilde{\eta}_{A_V}((1+2\mu)\cos^2\theta_A+(1+2\mu)\sin^2\theta_A))-\tilde{\eta}_{A_H}\tilde{\eta}_{B_H}$$
$$\Big(-2\sqrt{\mu(1+\mu)}\cos\theta_B\sin\theta_A-2\sqrt{\mu(1+\mu)}\cos\theta_A\sin\theta_B\Big)^2(2-\tilde{\eta}_{A_H}\tilde{\eta}_{A_H}((1+2\mu)\cos^2\theta_A$$
$$+(1+2\mu)\sin^2\theta_A))(2-\tilde{\eta}_{B_H}\tilde{\eta}_{B_H}((1+2\mu)\cos^2\theta_A+(1+2\mu)\sin^2\theta_A))\Big)\Big)\Big)+\sqrt{\tilde{\eta}_{A_H}}\sqrt{\tilde{\eta}_{B_H}}\Big(2\sqrt{\mu(1+\mu)}$$
$$\cos\theta_B\sin\theta_A-2\sqrt{\mu(1+\mu)}\cos\theta_A\sin\theta_B\Big)\Big(\sqrt{\tilde{\eta}_{A_V}}\sqrt{\tilde{\eta}_{A_H}}\sqrt{\tilde{\eta}_{B_V}}\sqrt{\tilde{\eta}_{B_H}}\Big(-2\sqrt{\mu(1+\mu)}\cos\theta_B\sin\theta_A$$
$$-2\sqrt{\mu(1+\mu)}\cos\theta_A\sin\theta_B\Big)\Big(2\sqrt{\mu(1+\mu)}\cos\theta_B\sin\theta_A+2\sqrt{\mu(1+\mu)}\cos\theta_A\sin\theta_B\Big)\sqrt{\tilde{\eta}_{A_V}}\sqrt{\tilde{\eta}_{B_V}}$$
$$\Big(2\sqrt{\mu(1+\mu)}\cos\theta_B\sin\theta_A-2\sqrt{\mu(1+\mu)}\cos\theta_A\sin\theta_B\Big)\sqrt{\tilde{\eta}_{A_H}}\sqrt{\tilde{\eta}_{B_H}}\Big(-2\sqrt{\mu(1+\mu)}\cos\theta_B\sin\theta_A$$
$$-2\sqrt{\mu(1+\mu)}\cos\theta_A\sin\theta_B\Big)\Big(\sqrt{\tilde{\eta}_{A_V}}\sqrt{\tilde{\eta}_{A_H}}\sqrt{\tilde{\eta}_{B_V}}\sqrt{\tilde{\eta}_{B_H}}\Big(-2\sqrt{\mu(1+\mu)}\cos\theta_B\sin\theta_A$$
$$-2\sqrt{\mu(1+\mu)}\cos\theta_A\sin\theta_B\Big)\Big(2\sqrt{\mu(1+\mu)}\cos\theta_B\sin\theta_A+2\sqrt{\mu(1+\mu)}\cos\theta_A\sin\theta_B\Big)$$
$$-\Big(\sqrt{\tilde{\eta}_{A_V}}\sqrt{\tilde{\eta}_{A_H}}\sqrt{\tilde{\eta}_{B_V}}\sqrt{\tilde{\eta}_{B_H}}\Big(2\sqrt{\mu(1+\mu)}\cos\theta_A\cos\theta_B-2\sqrt{\mu(1+\mu)}\sin\theta_A\sin\theta_B\Big)^2\Big)$$
$$-\sqrt{\tilde{\eta_{A_V}}}\sqrt{\tilde{\eta_{B_V}}}(2-\tilde{\eta_{A_H}}+\tilde{\eta_{A_H}}((1+2\mu)\cos^2\theta_A+(1+2\mu)\sin^2\theta_B))\Big(2\sqrt{\mu(1+\mu)}\cos\theta_B\sin\theta_A+$$
$$2\sqrt{\mu(1+\mu)}\cos\theta_A\sin\theta_B\Big)(2-\tilde{\eta_{B_H}}+\tilde{\eta_{B_H}}((1+2\mu)\cos^2\theta_B+(1+2\mu)\sin^2\theta_B))\Big)-\sqrt{\tilde{\eta}_{A_H}}\sqrt{\tilde{\eta}_{B_V}}$$
$$\Big(2\sqrt{\mu(1+\mu)}\cos\theta_A\cos\theta_B-2\sqrt{\mu(1+\mu)}\sin\theta_A\sin\theta_B\Big)\Big(\sqrt{\tilde{\eta}_{A_V}}\sqrt{\tilde{\eta}_{B_H}}\Big(2\sqrt{\mu(1+\mu)}\cos\theta_A\cos\theta_B$$
$$-2\sqrt{\mu(1+\mu)}\sin\theta_A\sin\theta_B\Big)\Big(\sqrt{\tilde{\eta}_{A_V}}\sqrt{\tilde{\eta}_{A_H}}\sqrt{\tilde{\eta}_{B_V}}\sqrt{\tilde{\eta}_{B_H}}\Big(-2\sqrt{\mu(1+\mu)}\cos\theta_B\sin\theta_A$$
$$-2\sqrt{\mu(1+\mu)}\cos\theta_A\sin\theta_B\Big)\Big(2\sqrt{\mu(1+\mu)}\cos\theta_B\sin\theta_A+2\sqrt{\mu(1+\mu)}\cos\theta_A\sin\theta_B\Big)\Big(\sqrt{\tilde{\eta}_{A_V}}\sqrt{\tilde{\eta}_{A_H}}$$
$$\sqrt{\tilde{\eta}_{B_V}}\sqrt{\tilde{\eta}_{B_H}}\Big(2\sqrt{\mu(1+\mu)}\cos\theta_A\cos\theta_B-2\sqrt{\mu(1+\mu)}\sin\theta_A\sin\theta_B\Big)^2\Big)+\sqrt{\tilde{\eta_{A_H}}}\sqrt{\tilde{\eta_{B_V}}}$$
$$(2-\tilde{\eta_{A_V}}+\tilde{\eta_{A_V}}((1+2\mu)\cos^2\theta_A+(1+2\mu)\sin^2\theta_A))\Big(2\sqrt{\mu(1+\mu)}\cos\theta_A\cos\theta_B-2\sqrt{\mu(1+\mu)}\sin\theta_A$$
$$\sin\theta_B\Big)(2-\tilde{\eta_{B_H}}+\tilde{\eta_{B_H}}((1+2\mu)\cos^2\theta_B+(1+2\mu)\sin^2\theta_B))\Big)+(2-\tilde{\eta_{B_V}}+\tilde{\eta_{B_V}}((1+2\mu)\cos^2\theta_B$$
$$+(1+2\mu)\sin^2\theta_B))\Big(-\tilde{\eta_{A_V}}\tilde{\eta_{B_H}}(2-\tilde{\eta_{A_H}}+\tilde{\eta_{A_H}}((1+2\mu)\cos^2\theta_A+(1+2\mu)\sin^2\theta_A))\Big(2\sqrt{\mu(1+\mu)}\cos\theta_A$$
$$\cos\theta_B-2\sqrt{\mu(1+\mu)}\sin\theta_A\sin\theta_B\Big)^2+(2-\tilde{\eta_{A_V}}+\tilde{\eta_{A_V}}((1+2\mu)\cos^2\theta_A+(1+2\mu)\sin^2\theta_A))$$

$$\Bigg(-\eta_{\tilde{A}_H}\eta_{\tilde{B}_H}\Bigg(-2\sqrt{\mu(1+\mu)}\cos\theta_B\sin\theta_A-2\sqrt{\mu(1+\mu)}\cos\theta_A\sin\theta_B\Bigg)^2+(2-\eta_{\tilde{A}_H}+\eta_{\tilde{A}_H}$$
$$((1+2\mu)\cos^2\theta_A+(1+2\mu)\sin^2\theta_A))(2-\eta_{\tilde{B}_H}+\eta_{\tilde{B}_H}((1+2\mu)\cos^2\theta_B+(1+2\mu)\sin^2\theta_B))\Bigg)\Bigg)\Bigg)$$
$$-\sqrt{\tilde{\eta}_{A_V}}\sqrt{\tilde{\eta}_{A_H}}\sqrt{\tilde{\eta}_{B_V}}\sqrt{\tilde{\eta}_{B_H}}\Bigg(-2\sqrt{\mu(1+\mu)}\cos\theta_A\cos\theta_B-2\sqrt{\mu(1+\mu)}\sin\theta_A\sin\theta_B\Bigg)^2$$
$$\Bigg(\sqrt{\tilde{\eta}_{A_V}}\sqrt{\tilde{\eta}_{B_V}}\Bigg(-2\sqrt{\mu(1+\mu)}\cos\theta_B\sin\theta_A-2\sqrt{\mu(1+\mu)}\cos\theta_A\sin\theta_B\Bigg)\sqrt{\tilde{\eta}_{A_H}}\sqrt{\tilde{\eta}_{A_V}}\sqrt{\tilde{\eta}_{B_H}}\sqrt{\tilde{\eta}_{B_V}}$$
$$\Bigg(-2\sqrt{\mu(1+\mu)}\cos\theta_B\sin\theta_A-2\sqrt{\mu(1+\mu)}\cos\theta_A\sin\theta_B\Bigg)\Bigg(2\sqrt{\mu(1+\mu)}\cos\theta_B\sin\theta_B$$
$$+2\sqrt{\mu(1+\mu)}\cos\theta_A\sin\theta_B\Bigg)-\sqrt{\tilde{\eta}_{A_H}}\sqrt{\tilde{\eta}_{A_V}}\sqrt{\tilde{\eta}_{B_H}}\sqrt{\tilde{\eta}_{B_V}}\Bigg(2\sqrt{\mu(1+\mu)}\cos\theta_A\cos\theta_B+2\sqrt{\mu(1+\mu)}$$
$$\sin\theta_A\sin\theta_B\Bigg)^2\Bigg)\sqrt{\tilde{\eta}_{A_V}}\sqrt{\tilde{\eta}_{B_V}}(2-\eta_{\tilde{A}_H}+\eta_{\tilde{A}_H}((1+2\mu)\cos^2\theta_A+(1+2\mu)\sin^2\theta_A))\Bigg(2\sqrt{\mu(1+\mu)}\cos\theta_B$$
$$\sin\theta_A+2\sqrt{\mu(1+\mu)}\cos\theta_A\sin\theta_B\Bigg)(2-\eta_{\tilde{B}_H}+\eta_{\tilde{B}_H}((1+2\mu)\cos^2\theta_B+(1+2\mu)\sin^2\theta_B))\Bigg)$$
$$-\sqrt{\tilde{\eta}_{A_H}}\sqrt{\tilde{\eta}_{B_V}}\Bigg(2\sqrt{\mu(1+\mu)}\cos\theta_A\cos\theta_B+2\sqrt{\mu(1+\mu)}\sin\theta_A\sin\theta_B\Bigg)\Bigg(\sqrt{\tilde{\eta}_{A_V}}\sqrt{\tilde{\eta}_{B_H}}$$
$$\Bigg(2\sqrt{\mu(1+\mu)}\cos\theta_A\cos\theta_B+2\sqrt{\mu(1+\mu)}\sin\theta_A\sin\theta_B\Bigg)\Bigg(\sqrt{\tilde{\eta}_{A_H}}\sqrt{\tilde{\eta}_{A_V}}\sqrt{\tilde{\eta}_{B_H}}\sqrt{\tilde{\eta}_{B_V}}$$
$$\Bigg(-2\sqrt{\mu(1+\mu)}\cos\theta_B\sin\theta_A-2\sqrt{\mu(1+\mu)}\cos\theta_A\sin\theta_B\Bigg)\Bigg(2\sqrt{\mu(1+\mu)}\cos\theta_B\sin\theta_A$$
$$+2\sqrt{\mu(1+\mu)}\cos\theta_A\sin\theta_B\Bigg)-\sqrt{\tilde{\eta}_{A_H}}\sqrt{\tilde{\eta}_{A_V}}\sqrt{\tilde{\eta}_{B_H}}\sqrt{\tilde{\eta}_{B_V}}\Bigg(2\sqrt{\mu(1+\mu)}\cos\theta_A\cos\theta_A-2\sqrt{\mu(1+\mu)}$$
$$\sin\theta_A\sin\theta_B\Bigg)^2\Bigg)+\sqrt{\tilde{\eta}_{A_H}}\sqrt{\tilde{\eta}_{B_V}}(2-\eta_{\tilde{A}_V}+\eta_{\tilde{A}_V}((1+2\mu)\cos^2\theta_A+(1+2\mu)\sin^2\theta_A))\Bigg(2\sqrt{\mu(1+\mu)}\cos\theta_B$$
$$\sin\theta_A+2\sqrt{\mu(1+\mu)}\cos\theta_A\sin\theta_B\Bigg)+(2-\eta_{\tilde{B}_V}+\eta_{\tilde{B}_V}((1+2\mu)\cos^2\theta_B+(1+2\mu)\sin^2\theta_B))-$$
$$\tilde{\eta}_{A_V}\tilde{\eta}_{B_V}\sqrt{\tilde{\eta}_{A_H}}\sqrt{\tilde{\eta}_{A_H}}(2-\eta_{\tilde{A}_H}+\eta_{\tilde{A}_H}((1+2\mu)\cos^2\theta_A+(1+2\mu)\sin^2\theta_A))\Bigg(2\sqrt{\mu(1+\mu)}\cos\theta_A\cos\theta_B+$$
$$2\sqrt{\mu(1+\mu)}\sin\theta_A\sin\theta_B\Bigg)^2+(2-\eta_{\tilde{A}_V}+\eta_{\tilde{A}_V}((1+2\mu)\cos^2\theta_A+(1+2\mu)\sin^2\theta_A))-$$
$$\tilde{\eta}_{A_H}\tilde{\eta}_{B_H}\Bigg(-2\sqrt{\mu(1+\mu)}\cos\theta_B\sin\theta_A-2\sqrt{\mu(1+\mu)}\cos\theta_A\sin\theta_B\Bigg)^2(2-\eta_{\tilde{A}_H}+\eta_{\tilde{A}_H}((1+$$
$$2\mu)\cos^2\theta_A+(1+2\mu)\sin^2\theta_A))(2-\eta_{\tilde{B}_H}+\eta_{\tilde{B}_H}((1+2\mu)\cos^2\theta_B+(1+2\mu)\sin^2\theta_B))\Bigg)\Bigg)\Bigg)\Bigg)\Bigg)$$
$$-\sqrt{\tilde{\eta}_{A_H}}\sqrt{\tilde{\eta}_{A_V}}\Bigg(-2\sqrt{\mu(1+\mu)}\cos\theta_A\cos\theta_B+2\sqrt{\mu(1+\mu)}\sin\theta_A\sin\theta_B\Bigg)\sqrt{\tilde{\eta}_{A_H}}\sqrt{\tilde{\eta}_{A_V}}$$

$$(2-\eta^{\tilde{}}_{A_V}+\eta^{\tilde{}}_{A_V}((1+2\mu)\cos^2\theta_A+(1+2\mu)\sin^2\theta_A))\Big(-2\sqrt{\mu(1+\mu)}\cos\theta_A\cos\theta_B$$
$$+2\sqrt{\mu(1+\mu)}\sin\theta_A\sin\theta_B\Big)(2-\eta^{\tilde{}}_{B_H}+\eta^{\tilde{}}_{B_H}((1+2\mu)\cos^2\theta_B+(1+2\mu)\sin^2\theta_B))\Big(\sqrt{\tilde{\eta}_{A_V}}\sqrt{\tilde{\eta}_{B_V}}$$
$$\Big(2\sqrt{\mu(1+\mu)}\cos\theta_B\sin\theta_A+2\sqrt{\mu(1+\mu)}\cos\theta_A\sin\theta_B\Big)\Big(\sqrt{\tilde{\eta}_{A_H}}\sqrt{\tilde{\eta}_{B_H}}\Big(-2\sqrt{\mu(1+\mu)}\cos\theta_B\sin\theta_A$$
$$-2\sqrt{\mu(1+\mu)}\cos\theta_A\sin\theta_B\Big)\Big(\sqrt{\tilde{\eta}_{A_H}}\sqrt{\tilde{\eta}_{A_V}}\sqrt{\tilde{\eta}_{B_H}}\sqrt{\tilde{\eta}_{B_V}}\Big(-2\sqrt{\mu(1+\mu)}\cos\theta_B\sin\theta_A$$
$$-2\sqrt{\mu(1+\mu)}\cos\theta_A\sin\theta_B\Big)\Big(2\sqrt{\mu(1+\mu)}\cos\theta_B\sin\theta_A+2\sqrt{\mu(1+\mu)}\cos\theta_A\sin\theta_B\Big)\sqrt{\tilde{\eta}_{A_H}}\sqrt{\tilde{\eta}_{A_V}}$$
$$\sqrt{\tilde{\eta}_{B_H}}\sqrt{\tilde{\eta}_{B_V}}\Big(2\sqrt{\mu(1+\mu)}\cos\theta_A\cos\theta_B-2\sqrt{\mu(1+\mu)}\sin\theta_A\sin\theta_B\Big)^2\Big)\sqrt{\tilde{\eta}_{A_V}}\sqrt{\tilde{\eta}_{B_V}}$$
$$(2-\eta^{\tilde{}}_{A_H}+\eta^{\tilde{}}_{A_H}((1+2\mu)\cos^2\theta_A+(1+2\mu)\sin^2\theta_A))\Big(2\sqrt{\mu(1+\mu)}\cos\theta_B\sin\theta_A+2\sqrt{\mu(1+\mu)}\cos\theta_A$$
$$\sin\theta_B\Big)(2-\eta^{\tilde{}}_{B_H}+\eta^{\tilde{}}_{B_H}((1+2\mu)\cos^2\theta_B+(1+2\mu)\sin^2\theta_B))\Big)-\sqrt{\tilde{\eta}_{A_H}}\sqrt{\tilde{\eta}_{B_V}}\Big(2\sqrt{\mu(1+\mu)}\cos\theta_A\cos\theta_B$$
$$-2\sqrt{\mu(1+\mu)}\sin\theta_A\sin\theta_B\Big)\Big(\sqrt{\tilde{\eta}_{A_V}}\sqrt{\tilde{\eta}_{B_H}}\Big(2\sqrt{\mu(1+\mu)}\cos\theta_A\cos\theta_B-2\sqrt{\mu(1+\mu)}\sin\theta_A\sin\theta_B\Big)$$
$$\Big(\sqrt{\tilde{\eta}_{A_H}}\sqrt{\tilde{\eta}_{A_V}}\sqrt{\tilde{\eta}_{B_H}}\sqrt{\tilde{\eta}_{B_V}}\Big(-2\sqrt{\mu(1+\mu)}\cos\theta_B\sin\theta_A-2\sqrt{\mu(1+\mu)}\cos\theta_A\sin\theta_B\Big)\Big(2\sqrt{\mu(1+\mu)}$$
$$\cos\theta_B\sin\theta_A+2\sqrt{\mu(1+\mu)}\cos\theta_A\sin\theta_B\Big)\sqrt{\tilde{\eta}_{A_H}}\sqrt{\tilde{\eta}_{A_V}}\sqrt{\tilde{\eta}_{B_H}}\sqrt{\tilde{\eta}_{B_V}}\Big(2\sqrt{\mu(1+\mu)}\cos\theta_A\cos\theta_B$$
$$-2\sqrt{\mu(1+\mu)}\sin\theta_A\sin\theta_B\Big)^2\Big)+\sqrt{\tilde{\eta}_{A_H}}\sqrt{\tilde{\eta}_{B_V}}(2-\eta^{\tilde{}}_{A_V}+\eta^{\tilde{}}_{A_V}((1+2\mu)\cos^2\theta_A+(1+2\mu)$$
$$\sin^2\theta_A))\Big(2\sqrt{\mu(1+\mu)}\cos\theta_A\cos\theta_B-2\sqrt{\mu(1+\mu)}\sin\theta_A\sin\theta_B\Big)(2-\eta^{\tilde{}}_{B_H}+\eta^{\tilde{}}_{B_H}((1$$
$$+2\mu)\cos^2\theta_B+(1+2\mu)\sin^2\theta_B))\Big)+(2-\eta^{\tilde{}}_{B_V}+\eta^{\tilde{}}_{B_V}((1+2\mu)\cos^2\theta_B+(1+2\mu)\sin^2\theta_B))-$$
$$\eta^{\tilde{}}_{A_V}\eta^{\tilde{}}_{B_H}(2-\eta^{\tilde{}}_{B_H}+\eta^{\tilde{}}_{B_H}((1+2\mu)\cos^2\theta_A+(1+2\mu)\sin^2\theta_A))\Big(2\sqrt{\mu(1+\mu)}\cos\theta_A\cos\theta_B-$$
$$2\sqrt{\mu(1+\mu)}\sin\theta_A\sin\theta_B\Big)^2(2-\eta^{\tilde{}}_{A_V}+\eta^{\tilde{}}_{A_V}((1+2\mu)\cos^2\theta_A+(1+2\mu)\sin^2\theta_A))\Big(-\eta^{\tilde{}}_{A_H}\eta^{\tilde{}}_{B_H}\Big(-$$
$$2\sqrt{\mu(1+\mu)}\cos\theta_B\cos\theta_B-2\sqrt{\mu(1+\mu)}\cos\theta_A\sin\theta_B\Big)2(2-\eta^{\tilde{}}_{A_H}+\eta^{\tilde{}}_{A_H}((1+2\mu)\cos^2\theta_A+$$
$$(1+2\mu)\sin^2\theta_A))(2-\eta^{\tilde{}}_{B_H}+\eta^{\tilde{}}_{B_H}((1+2\mu)\cos^2\theta_B+(1+2\mu)\sin^2\theta_B))\Big)\Big)\Big)+\sqrt{\eta^{\tilde{}}_{A_V}}\sqrt{\eta^{\tilde{}}_{B_H}}$$
$$\Big(-2\sqrt{\mu(1+\mu)}\cos\theta_A\cos\theta_B+2\sqrt{\mu(1+\mu)}\sin\theta_A\sin\theta_B\Big)\sqrt{\eta^{\tilde{}}_{A_H}}\sqrt{\eta^{\tilde{}}_{A_V}}\sqrt{\eta^{\tilde{}}_{B_H}}\sqrt{\eta^{\tilde{}}_{B_V}}$$
$$\Big(-2\sqrt{\mu(1+\mu)}\cos\theta_B\sin\theta_A-2\sqrt{\mu(1+\mu)}\cos\theta_A\sin\theta_B\Big)\Big(2\sqrt{\mu(1+\mu)}\cos\theta_B\sin\theta_A+$$

$$2\sqrt{\mu(1+\mu)}\cos\theta_A\sin\theta_B\Big)\Big(\sqrt{\eta^{\tilde{}}_{A_V}}\sqrt{\eta^{\tilde{}}_{B_V}}\Big(2\sqrt{\mu(1+\mu)}\cos\theta_B\sin\theta_A+2\sqrt{\mu(1+\mu)}\cos\theta_A\sin\theta_B\Big)$$
$$\sqrt{\eta^{\tilde{}}_{A_H}}\sqrt{\eta^{\tilde{}}_{B_H}}\Big(-2\sqrt{\mu(1+\mu)}\cos\theta_B\sin\theta_A-2\sqrt{\mu(1+\mu)}\cos\theta_A\sin\theta_B\Big)\Big(\sqrt{\eta^{\tilde{}}_{A_H}}\sqrt{\eta^{\tilde{}}_{A_V}}\sqrt{\eta^{\tilde{}}_{B_H}}\sqrt{\eta^{\tilde{}}_{B_V}}$$
$$\Big(-2\sqrt{\mu(1+\mu)}\cos\theta_B\sin\theta_A-2\sqrt{\mu(1+\mu)}\cos\theta_A\sin\theta_B\Big)\Big(2\sqrt{\mu(1+\mu)}\cos\theta_B\sin\theta_A+$$
$$2\sqrt{\mu(1+\mu)}\cos\theta_A\sin\theta_B\Big)-\sqrt{\eta^{\tilde{}}_{A_H}}\sqrt{\eta^{\tilde{}}_{A_V}}\sqrt{\eta^{\tilde{}}_{B_H}}\sqrt{\eta^{\tilde{}}_{B_V}}\Big(2\sqrt{\mu(1+\mu)}\cos\theta_A\cos\theta_B-2\sqrt{\mu(1+\mu)}$$
$$\sin\theta_A\sin\theta_B\Big)^2\Big)-\sqrt{\tilde{\eta}_{A_V}}\sqrt{\tilde{\eta}_{B_V}}(2-\eta^{\tilde{}}_{A_H}+\eta^{\tilde{}}_{A_H}((1+2\mu)\cos^2\theta_A+(1+2\mu)\sin^2\theta_A))\Big(2\sqrt{\mu(1+\mu)}\cos\theta_B$$
$$2\sqrt{\mu(1+\mu)}\cos\theta_A\sin\theta_B\Big)(2-\eta^{\tilde{}}_{B_H}+\eta^{\tilde{}}_{B_H}((1+2\mu)\cos^2\theta_B+(1+2\mu)\sin^2\theta_B))\Big)-\sqrt{\eta^{\tilde{}}_{A_H}}\sqrt{\eta^{\tilde{}}_{B_V}}$$
$$\Big(2\sqrt{\mu(1+\mu)}\cos\theta_A\cos\theta_B-2\sqrt{\mu(1+\mu)}\sin\theta_A\sin\theta_B\Big)\Big(\sqrt{\eta^{\tilde{}}_{A_V}}\sqrt{\eta^{\tilde{}}_{B_H}}\Big(2\sqrt{\mu(1+\mu)}\cos\theta_A\cos\theta_B-$$
$$2\sqrt{\mu(1+\mu)}\sin\theta_A\sin\theta_B\Big)\Big(\sqrt{\eta^{\tilde{}}_{A_H}}\sqrt{\eta^{\tilde{}}_{A_V}}\sqrt{\eta^{\tilde{}}_{B_H}}\sqrt{\eta^{\tilde{}}_{B_V}}\Big(-2\sqrt{\mu(1+\mu)}\cos\theta_B\sin\theta_A-2\sqrt{\mu(1+\mu)}$$
$$\cos\theta_A\sin\theta_B\Big)\Big(2\sqrt{\mu(1+\mu)}\cos\theta_B\sin\theta_A+2\sqrt{\mu(1+\mu)}\cos\theta_A\sin\theta_B\Big)-\sqrt{\eta^{\tilde{}}_{A_H}}\sqrt{\eta^{\tilde{}}_{A_V}}\sqrt{\eta^{\tilde{}}_{B_H}}\sqrt{\eta^{\tilde{}}_{B_V}}$$
$$\Big(2\sqrt{\mu(1+\mu)}\cos\theta_A\cos\theta_B-2\sqrt{\mu(1+\mu)}\sin\theta_A\sin\theta_B\Big)^2\Big)+\sqrt{\eta^{\tilde{}}_{A_H}}\sqrt{\eta^{\tilde{}}_{B_V}}(2-\eta^{\tilde{}}_{A_V}+\eta^{\tilde{}}_{A_V}((1+$$
$$2\mu)\cos^2\theta_A+(1+2\mu)\sin^2\theta_A))\Big(2\sqrt{\mu(1+\mu)}\cos\theta_A\cos\theta_B-2\sqrt{\mu(1+\mu)}\sin\theta_A\sin\theta_B\Big)(2-$$
$$\eta^{\tilde{}}_{B_H}+\eta^{\tilde{}}_{B_H}((1+2\mu)\cos^2\theta_B+(1+2\mu)\sin^2\theta_B))\Big)+(2-\eta^{\tilde{}}_{B_V}+\eta^{\tilde{}}_{B_V}((1+2\mu)\cos^2\theta_B+(1+$$
$$2\mu)\sin^2\theta_B))\Big)\Big(-\eta^{\tilde{}}_{A_V}\eta^{\tilde{}}_{B_H}(2-\eta^{\tilde{}}_{A_H}+\eta^{\tilde{}}_{A_H}((1+2\mu)\cos^2\theta_A+(1+2\mu)\sin^2\theta_A))\Big(2\sqrt{\mu(1+\mu)}\cos\theta_A$$
$$\cos\theta_B-2\sqrt{\mu(1+\mu)}\sin\theta_A\sin\theta_B\Big)^2(2-\eta^{\tilde{}}_{A_V}+\eta^{\tilde{}}_{A_V}((1+2\mu)\cos^2\theta_A+(1+2\mu)\sin^2\theta_A))\Big(-$$
$$\eta^{\tilde{}}_{A_H}\eta^{\tilde{}}_{B_H}\Big(-2\sqrt{\mu(1+\mu)}\cos\theta_B\sin\theta_A-2\sqrt{\mu(1+\mu)}\cos\theta_A\sin\theta_B\Big)^2+(2-\eta^{\tilde{}}_{A_H}+\eta^{\tilde{}}_{A_H}((1+$$
$$2\mu)\cos^2\theta_A+(1+2\mu)\sin^2\theta_A))(2-\eta^{\tilde{}}_{B_H}+\eta^{\tilde{}}_{B_H}((1+2\mu)\cos^2\theta_B+(1+2\mu)\sin^2\theta_B))\Big)\Big)\Big)-$$
$$\sqrt{\eta^{\tilde{}}_{A_H}}\sqrt{\eta^{\tilde{}}_{A_V}}\sqrt{\eta^{\tilde{}}_{B_H}}\sqrt{\eta^{\tilde{}}_{B_V}}$$
$$\Big(-2\sqrt{\mu(1+\mu)}\cos\theta_A\cos\theta_B-2\sqrt{\mu(1+\mu)}\sin\theta_A\sin\theta_B\Big)^2\Big(\sqrt{\eta^{\tilde{}}_{A_V}}\sqrt{\eta^{\tilde{}}_{B_V}}\Big(2\sqrt{\mu(1+\mu)}\cos\theta_B\sin\theta_A$$
$$+2\sqrt{\mu(1+\mu)}\cos\theta_A\sin\theta_B\Big)\Big(\sqrt{\eta^{\tilde{}}_{A_H}}\Big(\sqrt{\eta^{\tilde{}}_{A_V}}\Big(\sqrt{\eta^{\tilde{}}_{B_H}}\sqrt{\eta^{\tilde{}}_{B_V}}\Big(-2\sqrt{\mu(1+\mu)}\cos\theta_B\sin\theta_A-$$
$$2\sqrt{\mu(1+\mu)}\cos\theta_A\sin\theta_B\Big)\Big(2\sqrt{\mu(1+\mu)}\cos\theta_B\sin\theta_A+2\sqrt{\mu(1+\mu)}\cos\theta_A\sin\theta_B\Big)-\sqrt{\eta^{\tilde{}}_{A_H}}\sqrt{\eta^{\tilde{}}_{A_V}}$$

$$\sqrt{\eta_{\tilde{B}_H}}\sqrt{\eta_{\tilde{B}_V}}\Big(-2\sqrt{\mu(1+\mu)}\cos\theta_A\cos\theta_B-2\sqrt{\mu(1+\mu)}\sin\theta_A\sin\theta_B\Big)^2\Big)\sqrt{\eta_{\tilde{A}_V}}\sqrt{\eta_{\tilde{B}_V}}(2-\eta_{\tilde{A}_H}$$
$$+\eta_{\tilde{A}_H}((1+2\mu)\cos^2\theta_A+(1+2\mu)\sin^2\theta_A))\Big(2\sqrt{\mu(1+\mu)}\cos\theta_B\sin\theta_A+2\sqrt{\mu(1+\mu)}\cos\theta_A\sin\theta_B\Big)$$
$$(2-\eta_{\tilde{B}_H}+\eta_{\tilde{B}_H}((1+2\mu)\cos^2\theta_B+(1+2\mu)\sin^2\theta_B))\Big)-\sqrt{\eta_{\tilde{A}_H}}\sqrt{\eta_{\tilde{B}_V}}\Big(2\sqrt{\mu(1+\mu)}\cos\theta_A\cos\theta_B-$$
$$2\sqrt{\mu(1+\mu)}\sin\theta_A\sin\theta_B\Big)\sqrt{\eta_{\tilde{A}_V}}\sqrt{\eta_{\tilde{B}_H}}\Big(2\sqrt{\mu(1+\mu)}\cos\theta_A\cos\theta_B-2\sqrt{\mu(1+\mu)}\sin\theta_A\sin\theta_B\Big)$$
$$\Big(\sqrt{\eta_{\tilde{A}_H}}\sqrt{\eta_{\tilde{A}_V}}\sqrt{\eta_{\tilde{B}_H}}\sqrt{\eta_{\tilde{B}_V}}\Big(-2\sqrt{\mu(1+\mu)}\cos\theta_B\sin\theta_A-2\sqrt{\mu(1+\mu)}\cos\theta_A\sin\theta_B\Big)\Big(2\sqrt{\mu(1+\mu)}$$
$$\cos\theta_B\sin\theta_A+2\sqrt{\mu(1+\mu)}\cos\theta_A\sin\theta_B\Big)-\sqrt{\eta_{\tilde{A}_H}}\sqrt{\eta_{\tilde{A}_V}}\sqrt{\eta_{\tilde{B}_H}}\sqrt{\eta_{\tilde{B}_V}}\Big(2\sqrt{\mu(1+\mu)}\cos\theta_A\cos\theta_B-$$
$$2\sqrt{\mu(1+\mu)}\sin\theta_A\sin\theta_B\Big)^2\Big)+\sqrt{\eta_{\tilde{A}_H}}\sqrt{\eta_{\tilde{B}_V}}(2-\eta_{\tilde{A}_V}+\eta_{\tilde{A}_V}((1+2\mu)\cos^2\theta_A+(1+2\mu)\sin^2\theta_A))$$
$$\Big(2\sqrt{\mu(1+\mu)}\cos\theta_A\cos\theta_B-2\sqrt{\mu(1+\mu)}\sin\theta_A\sin\theta_B\Big)(2-\eta_{\tilde{B}_H}+\eta_{\tilde{B}_H}((1+2\mu)\cos^2\theta_B+$$
$$(1+2\mu)\sin^2\theta_B))\Big)+(2-\eta_{\tilde{B}_V}+\eta_{\tilde{B}_V}((1+2\mu)\cos^2\theta_B+(1+2\mu)\sin^2\theta_B))\Big(-\eta_{\tilde{A}_V}\eta_{\tilde{B}_H}(2-$$
$$\eta_{\tilde{A}_H}+\eta_{\tilde{A}_H}((1+2\mu)\cos^2\theta_A$$
$$+(1+2\mu)\sin^2\theta_A))\Big(2\sqrt{\mu(1+\mu)}\cos\theta_A\cos\theta_B-2\sqrt{\mu(1+\mu)}\sin\theta_A\sin\theta_B\Big)^2+(2-\eta_{\tilde{A}_V}+$$
$$\eta_{\tilde{A}_V}((1+2\mu)\cos^2\theta_A+(1+2\mu)\sin^2\theta_A))-\eta_{\tilde{A}_H}\eta_{\tilde{A}_V}\Big(2\sqrt{\mu(1+\mu)}\cos\theta_B\sin\theta_A-2\sqrt{\mu(1+\mu)}\cos\theta_A$$
$$\sin\theta_B\Big)^2+(2-\eta_{\tilde{A}_H}+\eta_{\tilde{A}_H}((1+2\mu)\cos^2\theta_A+(1+2\mu)\sin^2\theta_A))(2-\eta_{\tilde{B}_H}+\eta_{\tilde{B}_H}((1+$$
$$2\mu)\cos^2\theta_B+(1+2\mu)\sin^2\theta_B))\Big)\Big)\Big)\Big)\Big)+(2-\eta_{\tilde{B}_V}+\eta_{\tilde{B}_V}((1+2\mu)\cos^2\theta_B+(1+2\mu)\sin^2\theta_B))$$
$$\Big(-\eta_{\tilde{A}_V}\eta_{\tilde{B}_H}(2-\eta_{\tilde{A}_H}+\eta_{\tilde{A}_H}((1+2\mu)\cos^2\theta_A+(1+2\mu)\sin^2\theta_A))\Big(-2\sqrt{\mu(1+\mu)}\cos\theta_A\cos\theta_B+$$
$$2\sqrt{\mu(1+\mu)}\sin\theta_A\sin\theta_B\Big)^2\Big(\sqrt{\eta_{\tilde{A}_V}}\sqrt{\eta_{\tilde{B}_V}}\Big(2\sqrt{\mu(1+\mu)}\cos\theta_B\sin\theta_A+2\sqrt{\mu(1+\mu)}\cos\theta_A\sin\theta_B\Big)$$
$$\Big(\sqrt{\eta_{\tilde{A}_H}}\sqrt{\eta_{\tilde{B}_H}}\Big(-2\sqrt{\mu(1+\mu)}\cos\theta_B\sin\theta_A-2\sqrt{\mu(1+\mu)}\cos\theta_A\sin\theta_B\Big)\Big(\sqrt{\eta_{\tilde{A}_H}}\sqrt{\eta_{\tilde{A}_V}}\sqrt{\eta_{\tilde{B}_H}}\sqrt{\eta_{\tilde{B}_V}}$$
$$\Big(-2\sqrt{\mu(1+\mu)}\cos\theta_B\sin\theta_A-2\sqrt{\mu(1+\mu)}\cos\theta_A\sin\theta_B\Big)\Big(2\sqrt{\mu(1+\mu)}\cos\theta_B\sin\theta_A+$$
$$2\sqrt{\mu(1+\mu)}\cos\theta_A\sin\theta_B\Big)-\Big(\sqrt{\eta_{\tilde{A}_H}}\sqrt{\eta_{\tilde{A}_V}}\sqrt{\eta_{\tilde{B}_H}}\sqrt{\eta_{\tilde{B}_V}}\Big(-2\sqrt{\mu(1+\mu)}\cos\theta_A\cos\theta_A-$$
$$2\sqrt{\mu(1+\mu)}\sin\theta_A\sin\theta_B\Big)^2\Big)-\sqrt{\eta_{\tilde{A}_V}}\sqrt{\eta_{\tilde{B}_V}}(2-\eta_{\tilde{A}_H}+\eta_{\tilde{A}_H}((1+2\mu)\cos^2\theta_A+(1+2\mu)\sin^2\theta_A))$$

$$\left(2\sqrt{\mu(1+\mu)}\cos\theta_B\sin\theta_A+2\sqrt{\mu(1+\mu)}\cos\theta_A\sin\theta_B\right)(2-\eta_{\tilde{B}_H}+\eta_{\tilde{B}_H}((1+2\mu)\cos^2\theta_B+(1+2\mu)\sin^2\theta_B))\Bigg)-\Bigg(\sqrt{\eta_{\tilde{A}_H}}\sqrt{\eta_{\tilde{B}_V}}\left(2\sqrt{\mu(1+\mu)}\cos\theta_A\cos\theta_A-2\sqrt{\mu(1+\mu)}\sin\theta_A\sin\theta_B\right)\left(\sqrt{\eta_{\tilde{A}_V}}\sqrt{\eta_{\tilde{B}_H}}\left(2\sqrt{\mu(1+\mu)}\cos\theta_A\cos\theta_A-2\sqrt{\mu(1+\mu)}\sin\theta_A\sin\theta_B\right)\left(\sqrt{\eta_{\tilde{A}_H}}\sqrt{\eta_{\tilde{A}_V}}\sqrt{\eta_{\tilde{B}_H}}\sqrt{\eta_{\tilde{B}_V}}\left(-2\sqrt{\mu(1+\mu)}\cos\theta_B\sin\theta_A-2\sqrt{\mu(1+\mu)}\cos\theta_A\sin\theta_B\right)\left(2\sqrt{\mu(1+\mu)}\cos\theta_B\sin\theta_A+2\sqrt{\mu(1+\mu)}\cos\theta_A\sin\theta_B\right)-\sqrt{\eta_{\tilde{A}_H}}\sqrt{\eta_{\tilde{A}_V}}\sqrt{\eta_{\tilde{B}_H}}\sqrt{\eta_{\tilde{B}_V}}\left(-2\sqrt{\mu(1+\mu)}\cos\theta_A\cos\theta_B-2\sqrt{\mu(1+\mu)}\sin\theta_A\sin\theta_B\right)^2\right)+\sqrt{\eta_{\tilde{A}_H}}\sqrt{\eta_{\tilde{B}_V}}(2-\eta_{\tilde{A}_V}+\eta_{\tilde{A}_V}((1+2\mu)\cos^2\theta_A+(1+2\mu)\sin^2\theta_A))\left(2\sqrt{\mu(1+\mu)}\cos\theta_A\cos\theta_B-2\sqrt{\mu(1+\mu)}\sin\theta_A\sin\theta_B\right)(2-\eta_{\tilde{B}_H}+\eta_{\tilde{B}_H}((1+2\mu)\cos^2\theta_B+(1+2\mu)\sin^2\theta_B))\Bigg)+(2-\eta_{\tilde{B}_V}+\eta_{\tilde{B}_V}((1+2\mu)\cos^2\theta_B+(1+2\mu)\sin^2\theta_B))\Bigg(-\eta_{\tilde{A}_V}\eta_{\tilde{B}_H}(2-\eta_{\tilde{A}_H}+\eta_{\tilde{A}_H}((1+2\mu)\cos^2\theta_A+(1+2\mu)\sin^2\theta_A))\left(2\sqrt{\mu(1+\mu)}\cos\theta_A\cos\theta_B-2\sqrt{\mu(1+\mu)}\sin\theta_A\sin\theta_B\right)^2+(2-\eta_{\tilde{A}_V}+\eta_{\tilde{A}_V}((1+2\mu)\cos^2\theta_A+(1+2\mu)\sin^2\theta_A))\Bigg(-\eta_{\tilde{A}_H}\eta_{\tilde{B}_H}\left(-2\sqrt{\mu(1+\mu)}\cos\theta_B\sin\theta_A-2\sqrt{\mu(1+\mu)}\cos\theta_A\sin\theta_B\right)^2+(2-\eta_{\tilde{A}_H}+\eta_{\tilde{A}_H}((1+2\mu)\cos^2\theta_A+(1+2\mu)\sin^2\theta_A))(2-\eta_{\tilde{B}_H}+\eta_{\tilde{B}_H}((1+2\mu)\cos^2\theta_B+(1+2\mu)\sin^2\theta_B))\Bigg)\Bigg)\Bigg)+(2-\eta_{\tilde{A}_V}+\eta_{\tilde{A}_V}((1+2\mu)\cos^2\theta_A+(1+2\mu)\sin^2\theta_A))\Bigg(-\eta_{\tilde{A}_H}\eta_{\tilde{B}_H}\left(2\sqrt{\mu(1+\mu)}\cos\theta_B\sin\theta_A+2\sqrt{\mu(1+\mu)}\cos\theta_A\sin\theta_B\right)^2\Bigg(\sqrt{\eta_{\tilde{A}_V}}\sqrt{\eta_{\tilde{B}_V}}\left(2\sqrt{\mu(1+\mu)}\cos\theta_B\sin\theta_A+2\sqrt{\mu(1+\mu)}\cos\theta_A\sin\theta_B\right)\left(\sqrt{\eta_{\tilde{A}_H}}\sqrt{\eta_{\tilde{B}_H}}\left(-2\sqrt{\mu(1+\mu)}\cos\theta_B\sin\theta_A-2\sqrt{\mu(1+\mu)}\cos\theta_A\sin\theta_B\right)\left(\sqrt{\eta_{\tilde{A}_H}}\sqrt{\eta_{\tilde{A}_V}}\sqrt{\eta_{\tilde{B}_H}}\sqrt{\eta_{\tilde{B}_V}}\left(-2\sqrt{\mu(1+\mu)}\cos\theta_B\sin\theta_A-2\sqrt{\mu(1+\mu)}\cos\theta_A\sin\theta_B\right)\left(2\sqrt{\mu(1+\mu)}\cos\theta_B\sin\theta_A+2\sqrt{\mu(1+\mu)}\cos\theta_A\sin\theta_B\right)-\sqrt{\eta_{\tilde{A}_H}}\sqrt{\eta_{\tilde{A}_V}}\sqrt{\eta_{\tilde{B}_H}}\sqrt{\eta_{\tilde{B}_V}}\left(2\sqrt{\mu(1+\mu)}\cos\theta_A\cos\theta_B-2\sqrt{\mu(1+\mu)}\sin\theta_A\sin\theta_B\right)^2\right)-\sqrt{\eta_{\tilde{A}_V}}\sqrt{\eta_{\tilde{B}_V}}(2-\eta_{\tilde{A}_H}+\eta_{\tilde{A}_H}((1+2\mu)\cos^2\theta_A+(1+2\mu)\sin^2\theta_A))\left(2\sqrt{\mu(1+\mu)}\cos\theta_A\cos\theta_B+2\sqrt{\mu(1+\mu)}\sin\theta_A\sin\theta_B\right)(2-\eta_{\tilde{B}_H}+\eta_{\tilde{B}_H}((1+2\mu)\cos^2\theta_B+(1+2\mu)\sin^2\theta_B))\Bigg)-\sqrt{\eta_{\tilde{A}_H}}\sqrt{\eta_{\tilde{B}_V}}\left(2\sqrt{\mu(1+\mu)}\cos\theta_A\cos\theta_B-\right.$$

$$2\sqrt{\mu(1+\mu)}\sin\theta_A\sin\theta_B\Big)\Big(\sqrt{\eta^{\tilde{A}_V}}\sqrt{\eta^{\tilde{B}_H}}\Big(2\sqrt{\mu(1+\mu)}\cos\theta_A\cos\theta_B-2\sqrt{\mu(1+\mu)}\sin\theta_A\sin\theta_B\Big)$$
$$\Big(\sqrt{\eta^{\tilde{A}_H}}\sqrt{\eta^{\tilde{A}_V}}\sqrt{\eta^{\tilde{B}_H}}\sqrt{\eta^{\tilde{B}_V}}\Big(-2\sqrt{\mu(1+\mu)}\cos\theta_B\sin\theta_A-2\sqrt{\mu(1+\mu)}\cos\theta_A\sin\theta_B\Big)$$
$$\Big(2\sqrt{\mu(1+\mu)}\cos\theta_B\sin\theta_A+2\sqrt{\mu(1+\mu)}\cos\theta_A\sin\theta_B\Big)-\sqrt{\eta^{\tilde{A}_H}}\sqrt{\eta^{\tilde{A}_V}}\sqrt{\eta^{\tilde{B}_H}}\sqrt{\eta^{\tilde{B}_V}}$$
$$\Big(-2\sqrt{\mu(1+\mu)}\cos\theta_A\cos\theta_B-2\sqrt{\mu(1+\mu)}\sin\theta_A\sin\theta_B\Big)^2\Big)+\sqrt{\eta^{\tilde{A}_H}}\sqrt{\eta^{\tilde{B}_V}}(2-\eta^{\tilde{A}_V}+$$
$$\eta^{\tilde{A}_V}((1+2\mu)\cos^2\theta_A+(1+2\mu)\sin^2\theta_A))\Big(2\sqrt{\mu(1+\mu)}\cos\theta_A\cos\theta_B-2\sqrt{\mu(1+\mu)}\sin\theta_A\sin\theta_B\Big)$$
$$(2-\eta^{\tilde{B}_H}+\eta^{\tilde{B}_H}((1+2\mu)\cos^2\theta_B+(1+2\mu)\sin^2\theta_B))\Big)+(2-\eta^{\tilde{B}_V}+\eta^{\tilde{B}_V}((1+2\mu)\cos^2\theta_B+(1+$$
$$2\mu)\sin^2\theta_B))\Big(-\eta^{\tilde{A}_V}\eta^{\tilde{B}_H}(2-\eta^{\tilde{A}_H}+\eta^{\tilde{A}_H}((1+2\mu)\cos^2\theta_A+(1+2\mu)\sin^2\theta_A))\Big(2\sqrt{\mu(1+\mu)}\cos\theta_A\cos\theta_B$$
$$-2\sqrt{\mu(1+\mu)}\sin\theta_A\sin\theta_B\Big)^2(2-\eta^{\tilde{A}_V}+\eta^{\tilde{A}_V}((1+2\mu)\cos^2\theta_A+(1+2\mu)\sin^2\theta_A))\Big(-\eta^{\tilde{A}_H}\eta^{\tilde{B}_H}$$
$$\Big(-2\sqrt{\mu(1+\mu)}\cos\theta_B\sin\theta_A-2\sqrt{\mu(1+\mu)}\cos\theta_A\sin\theta_B\Big)^2(2-\eta^{\tilde{A}_H}+\eta^{\tilde{A}_H}((1+2\mu)\cos^2\theta_A+$$
$$(1+2\mu)\sin^2\theta_A))(2-\eta^{\tilde{B}_H}+\eta^{\tilde{B}_H}((1+2\mu)\cos^2\theta_B+(1+2\mu)\sin^2\theta_B))\Big)\Big)\Big)+(2-\eta^{\tilde{A}_H}+$$
$$\eta^{\tilde{A}_H}((1+2\mu)\cos^2\theta_A+(1+2\mu)\sin^2\theta_A))(2-\eta^{\tilde{B}_H}+\eta^{\tilde{B}_H}((1+2\mu)\cos^2\theta_B+(1+2\mu)\sin^2\theta_B))\Big(\sqrt{\eta^{\tilde{A}_V}}$$
$$\sqrt{\eta^{\tilde{B}_V}}\Big(2\sqrt{\mu(1+\mu)}\cos\theta_B\sin\theta_A+2\sqrt{\mu(1+\mu)}\cos\theta_A\sin\theta_B\Big)\Big(\sqrt{\eta^{\tilde{A}_H}}\sqrt{\eta^{\tilde{B}_H}}\Big(-2\sqrt{\mu(1+\mu)}\cos\theta_B$$
$$\sin\theta_A-2\sqrt{\mu(1+\mu)}\cos\theta_A\sin\theta_B\Big)\Big(\sqrt{\eta^{\tilde{A}_H}}\sqrt{\eta^{\tilde{A}_V}}\sqrt{\eta^{\tilde{B}_H}}\sqrt{\eta^{\tilde{B}_V}}\Big(-2\sqrt{\mu(1+\mu)}\cos\theta_B\sin\theta_A$$
$$-2\sqrt{\mu(1+\mu)}\cos\theta_A\sin\theta_B\Big)\Big(2\sqrt{\mu(1+\mu)}\cos\theta_B\sin\theta_A+2\sqrt{\mu(1+\mu)}\cos\theta_A\sin\theta_B\Big)-$$
$$\sqrt{\eta^{\tilde{A}_H}}\sqrt{\eta^{\tilde{A}_V}}\sqrt{\eta^{\tilde{B}_H}}\sqrt{\eta^{\tilde{B}_V}}\Big(2\sqrt{\mu(1+\mu)}\cos\theta_A\cos\theta_B-2\sqrt{\mu(1+\mu)}\sin\theta_A\sin\theta_B\Big)^2\Big)$$
$$-\sqrt{\eta^{\tilde{A}_V}}\sqrt{\eta^{\tilde{B}_V}}(2-\eta^{\tilde{A}_H}+\eta^{\tilde{A}_H}((1+2\mu)\cos^2\theta_A+(1+2\mu)\sin^2\theta_A))\Big(2\sqrt{\mu(1+\mu)}\cos\theta_B\sin\theta_A+$$
$$2\sqrt{\mu(1+\mu)}\cos\theta_A\sin\theta_B\Big)(2-\eta^{\tilde{B}_H}+\eta^{\tilde{B}_H}((1+2\mu)\cos^2\theta_B+(1+2\mu)\sin^2\theta_B))\Big)-\sqrt{\eta^{\tilde{A}_H}}\sqrt{\eta^{\tilde{B}_V}}$$
$$\Big(2\sqrt{\mu(1+\mu)}\cos\theta_A\cos\theta_B-2\sqrt{\mu(1+\mu)}\sin\theta_A\sin\theta_B\Big)\Big(\sqrt{\eta^{\tilde{A}_V}}\sqrt{\eta^{\tilde{B}_H}}\Big(2\sqrt{\mu(1+\mu)}\cos\theta_A\cos\theta_B-$$
$$2\sqrt{\mu(1+\mu)}\sin\theta_A\sin\theta_B\Big)\Big(\sqrt{\eta^{\tilde{A}_H}}\sqrt{\eta^{\tilde{A}_V}}\sqrt{\eta^{\tilde{B}_H}}\sqrt{\eta^{\tilde{B}_V}}\Big(-2\sqrt{\mu(1+\mu)}\cos\theta_B\sin\theta_A-2\sqrt{\mu(1+\mu)}$$
$$\cos\theta_A\sin\theta_B\Big)\Big(2\sqrt{\mu(1+\mu)}\cos\theta_B\sin\theta_A+2\sqrt{\mu(1+\mu)}\cos\theta_A\sin\theta_B\Big)-\sqrt{\eta^{\tilde{A}_H}}\sqrt{\eta^{\tilde{A}_V}}\sqrt{\eta^{\tilde{B}_H}}\sqrt{\eta^{\tilde{B}_V}}$$

$$\left(2\sqrt{\mu(1+\mu)}\cos\theta_A\cos\theta_B-2\sqrt{\mu(1+\mu)}\sin\theta_A\sin\theta_B\right)^2\Big)+\sqrt{\eta_{\tilde{A}_H}}\sqrt{\eta_{\tilde{B}_V}}(2-\eta_{\tilde{A}_V}+\eta_{\tilde{A}_V}((1+2\mu)\cos^2\theta_A+(1+2\mu)\sin^2\theta_A))\Big(2\sqrt{\mu(1+\mu)}\cos\theta_A\cos\theta_B-2\sqrt{\mu(1+\mu)}\sin\theta_A\sin\theta_B\Big)(2-\eta_{\tilde{B}_H}+\eta_{\tilde{B}_H}((1+2\mu)\cos^2\theta_B+(1+2\mu)\sin^2\theta_B))\Big)+(2-\eta_{\tilde{B}_V}+\eta_{\tilde{B}_V}((1+2\mu)\cos^2\theta_B+(1+2\mu)\sin^2\theta_B))\Big(-\eta_{\tilde{A}_V}\eta_{\tilde{B}_H}(2-\eta_{\tilde{A}_H}+\eta_{\tilde{A}_H}((1+2\mu)\cos^2\theta_A+(1+2\mu)\sin^2\theta_A))\Big(2\sqrt{\mu(1+\mu)}\cos\theta_A\cos\theta_B-2\sqrt{\mu(1+\mu)}\sin\theta_A\sin\theta_B\Big)^2+(2-\eta_{\tilde{A}_V}+\eta_{\tilde{A}_V}((1+2\mu)\cos^2\theta_A+(1+2\mu)\sin^2\theta_A))\Big(-\eta_{\tilde{A}_H}\eta_{\tilde{B}_H}(\Big(-2\sqrt{\mu(1+\mu)}\cos\theta_B\sin\theta_A-2\sqrt{\mu(1+\mu)}\cos\theta_A\sin\theta_B\Big)^2+(2-\eta_{\tilde{A}_H}+\eta_{\tilde{A}_H}((1+2\mu)\cos^2\theta_A+(1+2\mu)\sin^2\theta_A))(2-\eta_{\tilde{B}_H}+\eta_{\tilde{B}_H}((1+2\mu)\cos^2\theta_B+(1+2\mu)\sin^2\theta_B))\Big)\Big)\Big)\Big)\Big)$$

$$=64\Big(\eta_{\tilde{A}_H}(-2+\eta_{\tilde{B}_H}+\eta_{\tilde{B}_V})+\eta_{\tilde{A}_V}(\eta_{\tilde{B}_H}+\eta_{\tilde{B}_V})-2(\eta_{\tilde{A}_V}+\eta_{\tilde{B}_H}+\eta_{\tilde{B}_V}))\mu+(2\eta_{\tilde{B}_H}\eta_{\tilde{B}_V}+\eta_{\tilde{A}_V}(\eta_{\tilde{B}_H}+\eta_{\tilde{B}_V}-2\eta_{\tilde{B}_H}\eta_{\tilde{B}_V})+\eta_{\tilde{A}_H}(\eta_{\tilde{B}_H}+2\eta_{\tilde{A}_V}(-1+\eta_{\tilde{B}_H})(-1+\eta_{\tilde{B}_V})+\eta_{\tilde{B}_V}-2\eta_{\tilde{B}_H}\eta_{\tilde{B}_V}))\mu^2+(\eta_{\tilde{A}_H}-\eta_{\tilde{A}_V})(\eta_{\tilde{B}_H}-\eta_{\tilde{B}_V})\mu(1+\mu)\cos[2(\theta_A+\theta_B)]\Big)$$

### 4.0.2 Appendix B. General Program

```
mb = n;   % Here n = 1, 2, 3 ...

a[μ_, i_] := {{2 μ + 1, 0, 0, 2 √(μ (μ + 1))}, {0, 2 μ + 1, 2 √(μ (μ + 1)), 0},
   {0, 2 √(μ (μ + 1)), 2 μ + 1, 0}, {2 √(μ (μ + 1)), 0, 0, 2 μ + 1}}
b[μ_, i_] := {{2 μ + 1, 0, 0, -2 √(μ (μ + 1))}, {0, 2 μ + 1, -2 √(μ (μ + 1)), 0},
   {0, -2 √(μ (μ + 1)), 2 μ + 1, 0}, {-2 √(μ (μ + 1)), 0, 0, 2 μ + 1}}
p[μ_] = Normal[SparseArray@ArrayFlatten@
      Table[If[i == j, a[μ, i], 0], {i, (1 + mb)}, {j, (1 + mb)}]];
q[μ_] = Normal[SparseArray@ArrayFlatten@
      Table[If[i == j, b[μ, i], 0], {i, (1 + mb)}, {j, (1 + mb)}]];

gamma[μ_] := Normal[SparseArray[Band@{1, 1} → {p[μ], q[μ]}]]

gamma[μ] // MatrixForm;

SA[θ_] := {{Cos[θ], Sin[θ]}, {-Sin[θ], Cos[θ]}}
SB[φ_] := {{Cos[φ], Sin[φ]}, {-Sin[φ], Cos[φ]}}
SBS[i_] :=
 {{Divide[1, √2], 0, Divide[1, √2], 0}, {0, Divide[1, √2], 0, Divide[1, √2]},
  {Divide[-1, √2], 0, Divide[1, √2], 0}, {0, Divide[-1, √2], 0, Divide[1, √2]}}
p3[μ_] := Normal[SparseArray@
   ArrayFlatten@Table[If[i == j, SBS[i], 0], {i, (mb)}, {j, (mb)}]]
S[θ_, φ_] := Normal[SparseArray[Band@{1, 1} →
    {SA[θ], p3[μ], SB[φ], SA[θ], p3[μ], SB[φ]}]]

S[θ, φ] // MatrixForm;

Gamma1[μ_, θ_, φ_] := Transpose[S[θ, φ]].gamma[μ].S[θ, φ]

Gamma1[μ, θ, φ] // MatrixForm;

K1[η_, i_] := {{√η, 0}, {0, √η}}
α[η_, i_] := {{1 - η, 0}, {0, 1 - η}}
p2[η_, i_] := Normal[SparseArray@
   ArrayFlatten@Table[If[i == j, K1[η, i], 0], {i, (4 mb + 4)}, {j, (4 mb + 4)}]]
q2[η_, i_] := Normal[SparseArray@ArrayFlatten@
    Table[If[i == j, α[η, i], 0], {i, (4 mb + 4)}, {j, (4 mb + 4)}]]
alphaAB[η_] := Normal[SparseArray[Band@{1, 1} → {q2[η, i]}]]
K[η_] := Normal[SparseArray[Band@{1, 1} → {p2[η, i]}]]

S1 = Table[4 i - 1, {i, (mb + 1)}]; S2 = Table[4 i + 2, {i, mb}]; S3 = {1};
Clicks = Union[S2, S1, S3]; c = Subsets[Clicks, {1, Length[Clicks]}];

Q[μ_, θ_, φ_, η_] :=
 SetPrecision[Transpose[K[η]].Gamma1[μ, θ, φ].K[η] + alphaAB[η], Infinity]
```

```
Q[μ, θ, φ, η] // MatrixForm;

pmax[μ_, θ_, φ_, η_, v_] :=
 Total[Map[(x = Q[μ, θ, φ, η][[Join[#, # + (4 mb + 4)], Join[#, # + (4 mb + 4)]]];
       (-2 (1 - v))^Divide[Length[x], 2] / Sqrt[Det[x + IdentityMatrix[Length[x]]]]) &, c]] + 1

pmin[μ_, θ_, φ_, η_, v_] :=
 Total[Map[(x = Q[μ, θ, φ, η][[Join[#, # + (4 mb + 4)], Join[#, # + (4 mb + 4)]]];
       (-2 (1 - v))^Divide[Length[x], 2] / Sqrt[Det[x + IdentityMatrix[Length[x]]]]) &, c]] + 1

V[μ_] := (pmax[μ] - pmin[μ]) / (pmax[μ] + pmin[μ])

Plot[V[μ], {μ, 0, .2}, Exclusions → None, WorkingPrecision → 32]
```

# Bibliography


[1] Kwiat PG, Mattle K, Weinfurter H, Zeilinger A, Sergienko AV, Shih Y. New high-intensity source of polarization-entangled photon pairs. Physical Review Letters. 1995;75(24):4337.

[2] Gerry C, Knight P, Knight PL. Introductory quantum optics. Cambridge university press; 2005.

[3] Takeoka M, Jin RB, Sasaki M. Full analysis of multi-photon pair effects in spontaneous parametric down conversion based photonic quantum information processing. New Journal of Physics. 2015;17(4):043030.

[4] Wang XB, Hiroshima T, Tomita A, Hayashi M. Quantum information with Gaussian states. Physics reports. 2007;448(1-4):1–111.

[5] Einstein A, Podolsky B, Rosen N. Can quantum-mechanical description of physical reality be considered complete? Physical review. 1935;47(10):777.

[6] van Enk SJ, Hirota O. Entangled coherent states: Teleportation and decoherence. Physical Review A. 2001;64(2):022313.

[7] Hong CK, Ou ZY, Mandel L. Measurement of subpicosecond time intervals between two photons by interference. Physical review letters. 1987;59(18):2044.

[8] Louisell W, Yariv A, Siegman A. Quantum fluctuations and noise in parametric processes. I. Physical Review. 1961;124(6):1646.

[9] Hong C, Mandel L. Theory of parametric frequency down conversion of light. Physical Review A. 1985;31(4):2409.

[10] Jin ALE. ENTANGLED STATE PREPARATION FOR OPTICAL QUANTUM COMMUNICATION: Creating and characterizing photon pairs from Spontaneous Parametric Down Conversion inside bulk uniaxial crystals. PhD thesis, National University of Singapore; 2008.

[11] Sych D, Leuchs G. A complete basis of generalized Bell states. New Journal of Physics. 2009;11(1):013006.

[12] Shi BS, Tomita A. Generation of a pulsed polarization entangled photon pair using a Sagnac interferometer. Physical Review A. 2004;69(1):013803.

[13] Scherer A, Howard RB, Sanders BC, Tittel W. Quantum states prepared by realistic entanglement swapping. Physical Review A. 2009;80(6):062310.

[14] Khalique A, Tittel W, Sanders BC. Practical long-distance quantum communication using concatenated entanglement swapping. Physical Review A. 2013;88(2):022336.